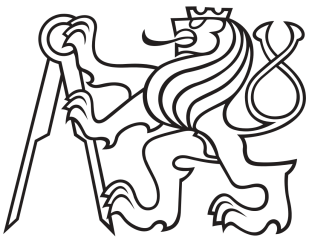

Czech Technical University in Prague
Faculty of Electrical Engineering
Department of Circuit Theory
Prague, 24.5.2024

Master's thesis

Comparison of fMRI analysis approaches for detecting group differences in the Self-agency experiment

Bc. Karolína Volfíková

Supervisor: Ing. Mgr. Jaroslav Hlinka, Ph.D.
Consultant: Ing. David Tomeček
Study program: Medical Electronics and Bioinformatics

MASTER‘S THESIS ASSIGNMENT

I. Personal and study details

Student's name: **Volfíková Karolína** Personal ID number: **491981**

Faculty / Institute: **Faculty of Electrical Engineering**

Department / Institute: **Department of Circuit Theory**

Study program: **Medical Electronics and Bioinformatics**

Specialisation: **Signal processing**

II. Master's thesis details

Master's thesis title in English:

Comparison of fMRI Analysis Approaches for Detecting Group Differences in the Self-agency Experiment

Master's thesis title in Czech:

Srovnání přístupů fMRI analýzy pro detekci skupinových rozdílů v experimentu Self-agency

Guidelines:

Schizophrenia is a psychiatric disorder that affects about one percent of the population. This chronic illness profoundly impacts the quality of life of the patient and his surroundings. One of the core markers of schizophrenia is a disturbance of the sense of self. Patients perceive some thoughts and actions of theirs to be under the control of an external agent. The project aims to optimize the methodology for statistical evaluation of the brain activation elicited by the Self-agency experiment [1], in order to improve its research and clinical utility in understanding schizophrenia, its diagnostic and particularly prognostic performance.
Project plan:
1. Familiarize yourself with literature concerning the experiment [1], the GIFT toolbox for data analysis.
2. Familiarize yourself with the research infrastructure at NUDZ and ICS, prepare the study sample(s) from dataset provided by the application partner (NUDZ).
3. Carry out a replication of the comparison study comparing the schizophrenia subjects with healthy controls - Spaniel et al. [1] - on an independent sample of a suitable size.
4. Propose alternative methods to analyze the data (using alternative explanatory variables: e.g. transitions instead/on top of the on/off blocks; using SPM, or analysis of functional connectivity of effective connectivity).
5. Design a principled approach for quantitative comparison of the analysis methods in terms of their predictive power (hint: switch from statistical testing approach to classification task).
6. Compare the performance of the models.
7. Bonus task: add regression model to explain the clinical symptoms at visit 1, and/or clinical symptoms/outcome at later visits.

Bibliography / sources:

[1] Spaniel, F., Tintera, J., Rydlo, J., Ibrahim, I., Kasparek, T., Horacek, J., Zaytseva, Y., Matejka, M., Fialova, M., Slovakova, A., Mikolas, P., Melicher, T., Görnerova, N., Höschl, C., & Hajek, T. (2016). Altered neural correlate of the self-agency experience in first-episode schizophrenia-spectrum patients: An fMRI study. Schizophrenia Bulletin, 42(4), 916–925. https://doi.org/10.1093/schbul/sbv188
[2] Daniel R. Weinberger and Paul J. Harrison, editors. Schizophrenia. Wiley, 12 2010
[3] V. D. Calhoun et al. A method for making group inferences using independent component analysis of functional MRI data: Exploring visual system. NeuroImage, S88, 2001
[4] Guo W., Yao D., Jiang J., et al. Abnormal default-mode network homogeneity in first-episode, drug-naive schizophrenia at rest. Prog Neuropsychopharmacol Biol Psychiatry. 2014;49:16-20

Name and workplace of master's thesis supervisor:

Ing. Mgr. Jaroslav Hlinka, Ph.D. Institute of Computer Science, The Czech Academy of Sciences, Prague

Name and workplace of second master's thesis supervisor or consultant:

Ing. David Tomeček National Institute of Mental Health, Klecany, Czech Republic

Date of master's thesis assignment: **15.02.2024** Deadline for master's thesis submission: **24.05.2024**

Assignment valid until: **21.09.2025**

Ing. Mgr. Jaroslav Hlinka, Ph.D. Supervisor's signature	doc. Ing. Radoslav Bortel, Ph.D. Head of department's signature	prof. Mgr. Petr Páta, Ph.D. Dean's signature

III. Assignment receipt

The student acknowledges that the master's thesis is an individual work. The student must produce her thesis without the assistance of others, with the exception of provided consultations. Within the master's thesis, the author must state the names of consultants and include a list of references.

.	
Date of assignment receipt	Student's signature

Declaration

I declare that the presented work was developed independently and that I have listed all sources of information used within it in accordance with the methodical instructions for observing the ethical principles in the preparation of university theses.

Prague, date 24.5.2024 Karolína Volfíková

Acknowledgements

I would like to express my gratitude to my thesis supervisor, Ing. Mgr. Jaroslav Hlinka, Ph.D., for his professional guidance, factual comments, and helpfulness during the completion of this thesis. My thanks also go to Ing. David Tomeček for valuable advice and professional insights. I would like to thank the Institute for Clinical and Experimental Medicine and the National Institute of Mental Health for providing the subjects' data necessary for the realization of the thesis.

Abstrakt

Self-agency experiment zkoumá jeden z hlavních příznaků schizofrenie, a to zkreslené vnímání sebe sama. V této práci jsou výsledky experimentu zanalyzovány pomocí analýzy nezávislých komponent a voxelové analýzy. Oba přístupy jsou dále porovnány z hlediska detekce rozdílů mezi skupinou pacientů se schizofrenií a skupinou zdravých kontrol a jsou použity v klasifikační úloze. Výsledky prokázaly významné rozdíly zejména v oblastech mediálního frontálního gyru, posteriorního cingulárního gyru a precuneu. Bylo zjištěno, že výsledky obou analýz jsou efektivní pro klasifikační úlohu, ale také že se výsledky liší při jejich použití na jiných nezávislých datasetech. Tato zjištění dopomohou lépe pochopit vnímání sebe sama u pacientů se schizofrenií, ale také přispívají k rozvoji využití těchto dat pro rozlišení zdravých subjektů a pacientů se schizofrenií.

Klíčová slova: schizofrenie, Self-agency experiment, analýza nezávislých komponent, statistické parametrické mapování, support vector machine

Abstract

The Self-agency experiment explores one of the main symptoms of schizophrenia, namely the distortion of self-perception. In this thesis, the results of the experiment are analyzed using the independent component analysis and the voxel-wise analysis. Both approaches are compared in terms of detecting differences between the group of schizophrenia patients and the group of healthy controls and are used in a classification task. Results proved significant differences especially in the areas of the medial frontal gyrus, posterior cingulate gyrus, and precuneus. It was found that the results of both analyses are effective for the classification, but also that they are different when applied to other independent datasets. These findings help to better understand the perception of self in schizophrenia patients and also contribute to the development of the use of these data for the differentiation between healthy and schizophrenia patients.

Key words: schizophrenia, Self-agency experiment, independent component analysis, statistical parametric mapping, support vector machine

List of abbreviations

FES	first-episode schizophrenia patients
HC	healthy controls
PANSS	positive and negative syndrome scale
ICA	independent component analysis
DMN	default mode network
CEN	central executive network
SPM	statistical parametric mapping
GLM	general linear model
SLIC	simple linear iterative clustering
PLS	partial least squares
SVM	support vector machine
SVR	support vector regression
fMRI	function magnetic resonance imaging
BOLD	blood-oxygen-level-dependent
IKEM	Institute for Clinical and Experimental Medicine
NIMH	National Institute of Mental Health
OA	other-agency
SA	self-agency

Contents

1 Motivation

Schizophrenia is a chronic psychiatric disorder that affects about one percent of the world's population [1]. It has a major negative effect on the patient's life and the lives of his family members [2]. Although schizophrenia has been researched by scientists for the past century, some of its processes and associated effects are still not fully understood.

The motivation behind this thesis is to help to a better understanding of this disorder and to provide insight into how the Self-agency experiment can be used for the classification of schizophrenia patients. This includes conducting a replication study of [3] by evaluating the independent component analysis and the voxel-wise analysis. The two approaches are then compared and used in a classification task in order to find out, whether any of them is efficient for the classification of schizophrenia patients based on the Self-agency experiment.

2 Theoretical foundations

2.1 Schizophrenia

Schizophrenia is a complex psychiatric disorder that profoundly affects the patient's processing of perception, emotion, and judgment. It changes the personality, experience, and perception of reality and impacts the ability to work as well as the social integration of the affected person [2]. The prevalence of schizophrenia is about 0.6 and 1.9%. The prevalence seems to be equal in males and females; in males, it usually occurs in their early 20s, and for women, it is usually in their late 20s or early 30s, and it is heritable [1]. From what has been found so far, it appears to be caused by a dysfunction of dopaminergic neurotransmission, variable involvement of several brain areas, and disturbances of synaptic functions [4].

Schizophrenia is a heterogeneous syndrome, and it manifests in many symptoms – there occur psychopathological changes such as delusions, loosening of connection of thoughts, hallucinations, and/or changes in behavior [1]. The characterization of symptoms is based on defining *positive* and *negative* symptoms. Positive symptoms, also referred to as psychotic symptoms are, e.g., suspiciousness, delusions, hallucinations, and grandiosity [5]. Negative symptoms include, e.g., diminished emotional expression and reaction, apathy, loss of energy and interest, social withdrawal [1]. The positive symptoms tend to relapse, and the negative and general tend to be chronic [4]. The symptoms can be evaluated using the PANSS scale [5], in which individual positive, negative, and also general psychopathology including depression and anxiety is captured.

One of the core markers of schizophrenia is the disturbance of the sense of self. Patients perceive some thoughts and actions to be under the control of an external agent. It has been confirmed that self-related processing is mediated by anterior and posterior cortical midline structures. The aberrant activity of underlying regions may result in feelings of thought insertion or delusions of control [3]. The delusions of control come from the pathology of the motor system. It seems that the actions move in one step from desire to execution with no control of the action. Even though these actions are being executed correctly, the affected

person does not feel in control [6].

This study works with patients with first-episode schizophrenia spectrum disorders (FES). Although the conceptual framework of schizophrenia by Kraepelin was set in 1919 [7], and schizophrenia has been the subject of research since, the precise nature, location, and origin of this disorder are still not certain. Nevertheless, accumulated knowledge suggests that already at the onset of symptoms, suggesting that the process of anatomical changes has been ongoing for several years, volumes of frontal and temporal areas are decreased in patients with schizophrenia [8]. However, these changes are not as pronounced as in chronic patients, and first-episode schizophrenia thus constitutes a window of opportunity for effective therapeutic interventions and predictions [9].

2.1.1 Regions of interest

While many brain regions have been reported to be affected in patients with schizophrenia, the current thesis focuses particularly on the alteration of the sense of agency. Thus, in this section, I review the core regions involved in this mental function.

The perception of self has been confirmed [10] to be mediated by cortical midline structures (CMS), especially anterior and posterior CMS (medial prefrontal cortex, anterior cingulate; posterior cingulate and precuneus). According to the prevailing view [10], the medial prefrontal cortex seems to account for the representation of self-related stimuli. Stimuli appear to be monitored in the anterior cingulate and evaluated in the dorsomedial prefrontal cortex. This can be integrated with the emotional and autobiographical context, and this is executed in the posterior cingulate cortex.

2.1.2 Functional brain networks

Functional brain networks can be detected using many approaches, e.g., the independent component analysis. [11] showed that up to 12 resting-state brain networks can be differentiated using the ICA.

In the context of self/other-agency, we are interested in activity, that can lead to the misattribution of the stimuli origin. Such aberrant activity can originate in central midline

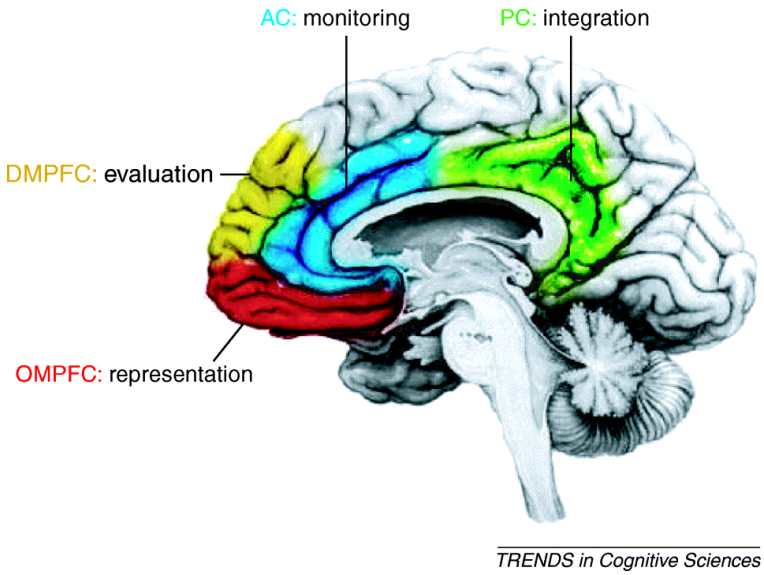

Figure 1: Processing of self-referential stimuli is concentrated in the cortical midline structures (CMS). Orbitomedial prefrontal cortex (OMPFC), dorsolateral prefrontal cortex (DMPFC), anterior cingulate cortex (AC), and posterior cingulate cortex (PC). Figure adapted from [10].

structures and related networks, such as the default mode network (DMN) [3]. The DMN is a brain network with properties that set it apart from the other brain systems. It exhibits the activation during mental explorations and thinking to oneself. It is linked with remembering, considering social interactions, and self-related events [12]. It comprises the dorsal medial prefrontal cortex, posterior cingulate cortex, precuneus, and angular gyrus [12].

2.2 Independent component analysis

2.2.1 Definition

Independent component analysis (ICA) is a method for finding a linear transformation of non-Gaussian data that minimizes the statistical dependence between its components [13]. It captures the essential structure of the data and can be used for feature extraction or signal separation [14].

Let $x_1, \ldots, x_n$ be n linear mixtures of n independent components ([13]):

$$x_j = a_{j_1} s_1 + ... + a_{j_n} s_n, \tag{1}$$

where s_n are the original (unknown) signals, x_n are the observed signals, and a_{j_n} are the (unknown) parameters to be estimated. This so-called cocktail-party problem can be solved by several approaches; ICA assumes that s_n are statistically independent, which allows estimating the parameters a_{j_n} and separating the signals.

In vector-matrix notation, we get $\mathbf{x}$ as the vector of mixtures $x_1, \ldots, x_n$, $\mathbf{s}$ as the random vector with elements $s_1, \ldots, s_n$. Then we denote by $\mathbf{A}$ the matrix with elements a_{j_n}. The ICA model of the mixture is then represented as

$$\mathbf{x} = \mathbf{A}\mathbf{s}. \tag{2}$$

The ICA model can be estimated when the following is satisfied:

1. Original signals $s_1 \ldots s_n$ are statistically independent.
2. Original signals $s_1 \ldots s_n$ have non-Gaussian distributions.
3. The matrix $\mathbf{A}$ is square.

The process of the model estimation itself can be summarized as estimating the matrix $\mathbf{A}$, then finding its inverse – let us denote it by $\mathbf{W}$ – and using it to obtain the independent components according to ([13]):

$$\mathbf{s} = \mathbf{W}\mathbf{x}. \tag{3}$$

In the case of fMRI analysis, ICA identifies prominent BOLD signal sources. The independent components are then used to construct spatial maps and the corresponding time courses. A spatial map represents the distribution of a specific component across the brain's voxel space. It highlights the regions where the component was the most influential. Then, the time course of an independent component represents the temporal dynamics associated with a specific spatial map.

2.2.2 Algorithms for ICA estimation

FastICA The assumption of non-Gaussianity can be used as a principal in ICA estimation. A commonly used measure of Gaussianity is the fourth standardized moment, i.e., kurtosis. For a random variable y, kurtosis is defined as:

$$kurt(y) = E\{y^4\} - 3(E\{y^2\})^2. \tag{4}$$

And since the fourth moment for y with a Gaussian distribution equals $3(E\{y^2\})^2$, the kurtosis is zero for a Gaussian random variable. For most non-Gaussian random variables, kurtosis is non-zero [14].

Another measure of Gaussianity is *negentropy*. Since variables that have Gaussian distribution have the largest entropy among all random variables of equal variance, negentropy was designed to provide the opposite. It is a modification of the entropy calculation and is equal to zero for Gaussian variables and is positive for Gaussian variables. The entropy of a continuous random variable y follows the equation [15]:

$$H(y) = -\int f(y) \log f(y) dy, \tag{5}$$

where $f(y)$ is the density of y. Negentropy is then defined as:

$$J(y) = H(y_g) - H(y), \tag{6}$$

where y_g is a Gaussian random variable with the same covariance matrix as y.

Infomax Mutual information serves as a measure of dependence between two random variables. Its definition uses the above-described entropy. When $\mathbf{y}$ is a vector of random variables, the mutual information between the variables y_i holds:

$$I(y_1, y_2, \ldots, y_n) = \sum_{i=1}^{n} H(y_i) - H(y). \tag{7}$$

I is zero if and only if the variables are statistically independent, and is always non-negative. Thus, it can be used as a criterion for ICA estimation. The transformation matrix $\mathbf{W}$ in the eq. 3 is, in this case, found by minimization of mutual information of s_i [16].

Another approach for ICA estimation is maximum likelihood estimation. This approach is essentially equivalent to already-described minimization of mutual information [14].

2.2.3 ICASSO

The application of ICA brings several problems. One of the key issues is that the optimization can get stuck in local minima. Since the convergence to the global minima is not guaranteed, it leads to low reliability of the estimated independent components. ICASSO is a method that runs the ICA algorithm several times with differently bootstrapped data sets or different initial values. It provides an insight into the reliability of components – reliable estimates correspond to tight clusters and unreliable ones to points that do not belong to any such cluster. A commonly used decision boundary for determining component stability is the stability index (SI) equal to 0.9. Above this threshold (0.9 included), the component is considered stable [17].

2.3 Statistical Parametric Mapping

Statistical Parametric Mapping (SPM) is a statistical technique used to identify regionally specific effects in neuroimaging data [18]. It uses a voxel-based approach to describe significant changes in activity over time during various experimental factors. SPM involves data preprocessing, usually realignment, and normalization into some standard anatomical space, described in more detail in [18].

SPM connects the general linear model (GLM) and random field theory (RFT) when GLM is used to estimate parameters explaining the data, and RFT is used to resolve the multiple comparison problem. The general linear model is defined as:

$$Y = \beta_0 + \beta_1 X_1 + \beta_2 X_2 + \ldots + \beta_p X_p + \epsilon, \tag{8}$$

The observed response variable Y is expressed as a linear combination of explanatory variables X and an error ϵ. The matrix that contains the explanatory variables is called the *design matrix*. Its columns are also referred to as regressors. In terms of an experiment analysis, the

regressors can represent different conditions of the experiment. Each column of the design matrix has an associated unknown parameter β_x. As it is partially shown in Figure 2, the design matrix includes condition-specific effects but also confounding effects and constant term.

Retrieved regressors and their coefficients can be used to run a range of statistical analyses. E.g. to test the null hypothesis, that some linear combination of the estimates is zero, using t-test. The statistic is obtained by using *contrasts* – weight vectors – to compare the difference in responses to conditions.

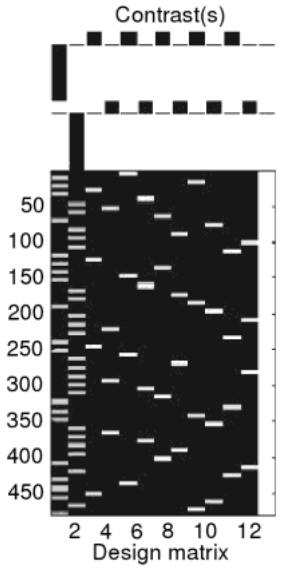

Figure 2: Image representation of the design matrix addapted from [18]. Contrasts are the vectors of weights defining which compounds of parameters are tested.

2.4 SLIC superpixels

Simple linear iterative clustering (SLIC) is a clustering algorithm that generates superpixels by clustering pixels based on their color similarity and proximity in the image plane [19]. The process is performed in the five-dimensional space given by CIELAB color space *[lab]* and pixel coordinates *[xy]*. The authors of the algorithm introduce a distance measure, that enforces

color similarity as well as pixel proximity. The distance $D_s(i,k)$ between two points i,k with coordinates $i = (l_i, a_i, b_i, x_i, y_i)$ and $k = (l_k, a_k, b_k, x_k, y_k)$ is given by [19]:

$$\begin{aligned} D_s &= d_{lab} + \frac{m}{S} d_{xy} \\ d_{lab} &= \sqrt{(l_k - l_i)^2 + (a_k - a_i)^2 + (b_k - b_i)^2} \\ d_{xy} &= \sqrt{(x_k - x_i)^2 + (y_k - y_i)^2}, \end{aligned} \tag{9}$$

where the variable m is introduced as the *compactness* parameter (the greater the value, the more spatial proximity outweighs the color proximity). D_s is thus the sum of the *lab* and *xy* plane distance normalized by the grid interval S. The grid interval is defined by the number of desired clusters K (given by the user) and the number of pixels N in the image $S = \sqrt{N/K}$.

At the onset of the algorithm, the number of clusters, i.e., the number of cluster centers at regular grid intervals S, is chosen. The search area for each cluster center is then defined by its $2S \times 2S$ neighborhood area. Then, each pixel in the image is associated with the nearest cluster center. When all the pixels are associated, new centers are computed as the average of all the pixels belonging to the cluster. The process is iteratively repeated until convergence [19].

2.5 Partial Least Squares

Partial Least Squares (PLS) is a supervised learning method used to find latent variables (components) that are linear combinations of the input variables ($\mathbf{X}$) and the output variables ($\mathbf{Y}$) [20]. It is used to transform the original predictors into lower-dimensional space. In comparison to another commonly used method of dimensionality reduction, PCA, which finds a transformation such that it explains the maximum variance in $\mathbf{X}$, PLS maximizes the covariance between the $\mathbf{X}$ and $\mathbf{Y}$ [21].

The general formulation of PLS in matrix notation is as follows [20]:

$$\begin{aligned} \mathbf{X} &= \mathbf{T}\mathbf{P}^{\mathbf{T}} + \mathbf{E} \\ \mathbf{Y} &= \mathbf{U}\mathbf{Q}^{\mathbf{T}} + \mathbf{F}, \end{aligned} \tag{10}$$

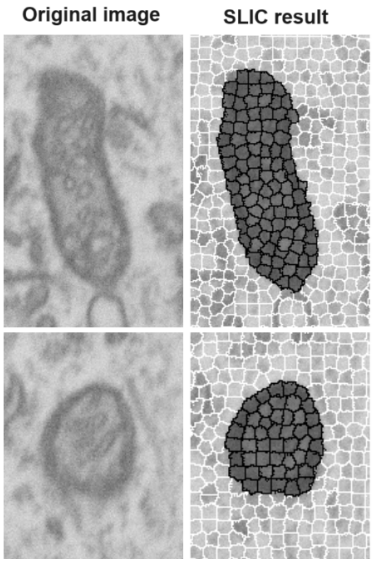

Figure 3: Example of an image segmented using the SLIC algorithm into superpixels. Figure adapted from [19]

where $\mathbf{T}, \mathbf{U}$ are projections of $\mathbf{X}, \mathbf{Y}$, $\mathbf{P}, \mathbf{Q}$ are loading matrices and $\mathbf{E}, \mathbf{F}$ are the error terms. The solution of PLS then is based on singular value decomposition.

Note that the above-described method is used when X is a set of independent variables and $\mathbf{Y}$ is a set of dependent variables. When Y is a set of categorical response variables (labels), there applies the variation of PLS, i.e., PLS-DA, Partial Least Squares-Discriminant Analysis [22].

2.6 Support Vector Machine

Support vector machine (SVM) is a supervised machine learning algorithm used for both classification and regression tasks [23]. The algorithm finds an optimal hyperplane with the consideration of a *margin*, that is defined depending on the nature of the task – whether it is a classification or regression problem.

2.6.1 Classification

Support vector machine algorithm for classification finds a hyperplane that maximizes the distance of data points of the classes. Let

$$\mathbf{w} \cdot \mathbf{x} + b = 0 \tag{11}$$

be a linear classifier given by parameters $(\mathbf{w}, b)$, $\mathbf{w}$ is normal to the hyperplane given by the classifier, $|b|/\|\mathbf{w}\|$ is the perpendicular distance from the hyperplane to the origin. $\mathbf{x}$ is a vector of training data, each belonging to either positive or negative class: $\{\mathbf{x}_i, y_i\}$, $i = 1, \ldots, l$; $y_i \in \{-1, 1\}$; $\mathbf{x}_i \in \mathbf{R}^d$. The *margin* m of the hyperplane is defined as the sum of the shortest distances from the hyperplane to the closest positive (d_+)/negative (d_-) data point [24]:

$$m = d_+ + d_-; \quad \text{sign}(d(\mathbf{x}, y)) = \frac{y(\mathbf{w} \cdot \mathbf{x} + b)}{\|\mathbf{w}\|}. \tag{12}$$

The SVM algorithm looks for the separating hyperplane with the largest margin. The problem (for separable data) can be formulated as [24] [23]:

$$y_i(\mathbf{x}_i \cdot \mathbf{w} + b) - 1 \geq 0 \quad \forall i. \tag{13}$$

Since the two hyperplanes H_1, H_2 defining the borders of the margin m are parallel, we get to the simplification: $\text{sign}(d) = 1/\|\mathbf{w}\|$. Hence the margin

$$m = 2/\|\mathbf{w}\|. \tag{14}$$

The optimization formulation for the maximum margin m^* is a quadratic programming problem defined as:

$$\begin{aligned} m^* = (\mathbf{w}^*, b^*) = \max_{\mathbf{w},b} \frac{2}{\|\mathbf{w}\|} = \min_{\mathbf{w},b} \frac{1}{2}\|\mathbf{w}\|^2, \\ s.t. : y(\mathbf{w} \cdot \mathbf{x} + b) \geq 1, \quad \forall (\mathbf{x}, y). \end{aligned} \tag{15}$$

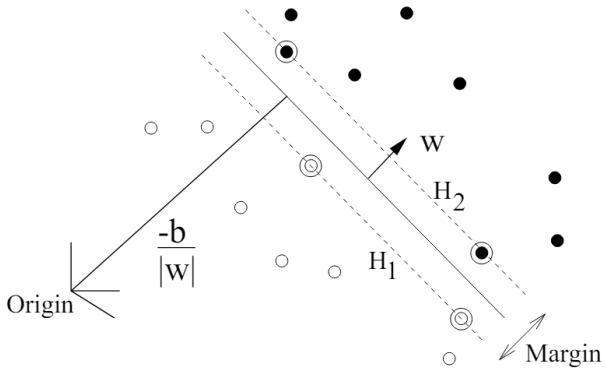

Figure 4: Linear separating hyperplanes for separable data. The support vectors are circled. Figure was adapted from [25].

Non-separability of the data If the data are linearly separable with some noise, the algorithm is extended with *slack variables* ξ_i. If the data point does not fulfill the condition $y(\mathbf{w}\cdot\mathbf{x}+b)\geq 1$, the condition is relaxed to $y(\mathbf{w}\cdot\mathbf{x}+b)\geq 1-\xi$ and penalty $C\cdot\xi$ is paid. The problem formulation is changed to:

$$\begin{aligned}(\mathbf{w}^*,b^*) &= \min_{\mathbf{w},b}\frac{1}{2}\|\mathbf{w}\|^2 + C\sum_{i=1}^{N}\xi_i,\\ s.t.: y_i(\mathbf{w}\cdot\mathbf{x}_i+b) &\geq 1-\xi_i,\\ \xi_i &\geq 0,\\ \forall i &= 1,\ldots,N.\end{aligned} \tag{16}$$

If the data are not linearly separable, the data can be mapped to a higher-dimensional space by a nonlinear transformation, where it becomes linearly separable. Find more details in [23].

2.6.2 Regression

Support vector regression (SVR) uses the same concept of fitting a hyperplane using a margin as a criterion. The difference is in the definition of the margin – in SVR, the margin is a *error tolerance* of the model, which allows the data points to be deviated from the hyperplane

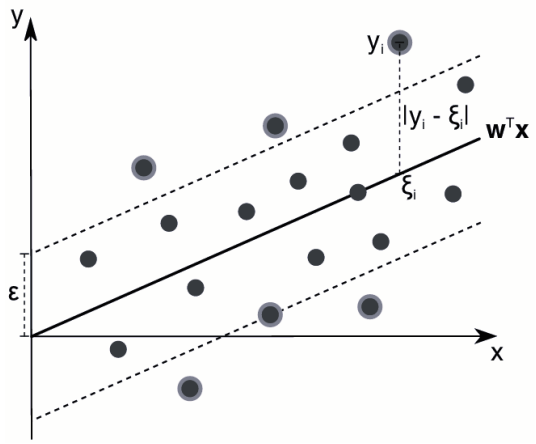

Figure 5: Linear support vector regression example. The given example is a non-feasible case, the *slack variables* ξ_i are introduced. The support vectors are circled. [27]

and not counted as errors if they are inside the margin. The objective function stays the same; the change is visible in the constraints [26]:

$$\begin{aligned} (\mathbf{w}^*, b^*) &= \min_{\mathbf{w},b} \frac{1}{2}\|\mathbf{w}\|^2, \\ s.t. : y_i - \mathbf{w} \cdot \mathbf{x}_i - b &\leq \epsilon \\ \mathbf{w} \cdot \mathbf{x}_i + b - y_i &\leq \epsilon \end{aligned} \tag{17}$$

where ϵ is the deviation of the model from the targets.

Equation 17 describes the basic idea of SVR and holds for feasible problems. The case of non-feasibility can be solved with similar methods as in the case of classification tasks. There can be *slack variables* introduced to allow for some errors with a penalty, or the data can be transformed to higher-dimensional space [26].

3 Data and methodology

In my thesis, I first conduct a replication study in which I try to verify the results of Spaniel and others [3] using independent component analysis (ICA) and the voxel-wise analysis. The study is not replicated exactly, in some parts, the methodology is modified due to unnecessary complexity in the original study (particularly analyzing stimulation blocks separately), which led to lower interpretability of the results. In the study, authors compared neural activity in patients with first-episode schizophrenia-spectrum disorders (FES) and healthy controls (HC). The functional connectivity during the Self-agency experiment was analyzed using ICA. Results showed lower cortical activation of the medial frontal gyrus and posterior cingulate gyrus in FES compared to HC. They also reported that the self/other-agency judgment is related to the dynamic switching of the default mode network (DMN) and the central executive network (CEN). After replication of the ICA analysis, I complement the results by voxel-wise analysis and compare the outcomes.

Notably, the replication is further extended by applying the machine learning approach. In particular, both analyses' results are further used in a classification (FES/HC) and regression (clinical symptom severity) task. The replication and the classification task are subsequently performed on an independent dataset from a different MRI center, to assess reproducibility of the results.

3.1 Data collection

Subjects whose data are used in this study were evaluated with MINI Internation Neuropsychiatric Interview [28]. The exclusion criteria included a history of seizures or significant head trauma, mental retardation, a history of substance addiction, and MRI contraindications. First-episode schizophrenia patients (FES) were at the initial stage of second-generation antipsychotic therapy. Healthy subjects (HC) did not have any major psychiatric disorder in their past or family history. All subjects were right-handed.

3.1.1 Replication study and classification task

In the study of Spaniel and others [3], the data consisted of thirty-five FES patients and thirty-five HC. For replication, I have a larger sample available – it consists of 81 schizophrenia patients and 55 controls, in total 136 subjects (more details are listed in Table 1). Subjects from the previous study are included in the enlarged sample to provide a larger dataset for the classification task. Validation of the methods and classifier is then performed on a different, independent dataset.

group	**n**	**age: mean**	**age: std**
FES, M	41	28.6	7.3
FES, F	40	30.2	7.2
HC, M	24	26.6	5.2
HC, F	31	25.2	3.6

Table 1: Table of representation of groups FES and HC, males (M) and females (F) in the IKEM dataset. n column specifies the number of subjects, in the columns *age: mean* and *age: std* are the group's mean age and the standard deviation of age.

All subjects underwent the Self-agency experiment in the Institute for Clinical and Experimental Medicine (IKEM) while their brain activity was measured using the same magnetic resonance machine – 3 Tesla Siemens Trio scanner equipped with a 12-channel head coil. Functional images were obtained using the T2-weighted gradient echo-planar imaging sequence sensitive to the blood oxygenation level-dependent (BOLD) signal with parameters: repetition time (TR) of 2000 ms, echo time (TE) 30 ms, flip angle 90°, voxel size $3 \times 3 \times 3\, mm^3$, field of view (FOV) 192×192 mm, matrix size 64×64, each volume with 30 axial slices (slice order: sequential decreasing), 240 volumes in total.

3.1.2 Testing on an independent dataset

In addition to the dataset from IKEM, the analyses and the classification task are also performed on another separate dataset obtained from the National Institute of Mental Health

(NIHM). The dataset contains 165 subjects: 97 FES patients and 68 HC; more details are listed in Table 2. Subjects underwent the same experiment, the only difference being the MRI machine, which was a 3 Tesla Siemens Prisma scanner equipped with a standard 64-channel/20-channel head coil. Functional images were obtained using the T2-weighted (T2) gradient echo-planar imaging sequence sensitive to the BOLD signal. Parameters of the sequence were: TR of 2000 ms, TE 30 ms, flip angle 90°, voxel size $3 \times 3 \times 3\,mm^3$, field of view (FOV) 192×192 mm, matrix size 64×64, each volume with 30 axial slices (slice order: alternating increasing), 240 volumes in total. Note that while the parameters were kept intentionally the same (apart from the order of slice acquisition), the difference in the scanner and head coil is likely to affect the signal parameters; in general, the NIHM dataset should have a better signal-to-noise (SNR) ratio, however, it can also be differentially affected by various artifacts.

group	**n**	**age: mean**	**age: std**
FES, M	59	27.5	7.2
FES, F	38	30.4	7.3
HC, M	27	32.0	5.3
HC, F	41	31.8	9.8

Table 2: Table of representation of groups FES and HC, males (M) and females (F) in the NIHM dataset. *n* column specifies the number of subjects, in the columns *age: mean* and *age: std* are the group's mean age and the standard deviation of age.

3.2 Self-agency experiment

All research in the context of this thesis is based on the self and other-agency judgment during a specifically designed experiment. During fMRI, stimuli in the form of a moving cursor in a square, as shown in Figure 6, are presented to the subject. Subjects are instructed to move the cursor using a joystick to the outer corridor if they believe the cursor's movement is fully under their control and to move the cursor to the center of the square if they feel

like the experimenter influences the cursor movement. In reality, the cursor is not influenced by the experimenter, but its motion is during selected experimental blocks (time segments) driven by software that introduces angular distortions.

The paradigm consists of 24 blocks – 12 blocks of other-agency (OA) and 12 blocks of self-agency (SA). Blocks are in an alternating sequence, each block lasting 20 seconds. Throughout the OA blocks, the cursor movement is influenced by the software-based angular distortions. Throughout the SA blocks, the cursor movement exactly matches the joystick movement initiated by the subject.

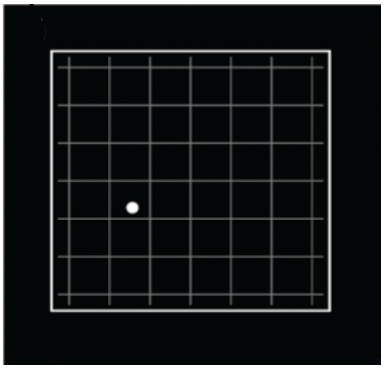

Figure 6: Illustrative screenshot example of the display projected in fMRI during the Self-agency experiment [3].

For the purposes of fMRI analysis in this study, the paradigm is simulated as a series of zeros (in the case of the OA condition) and ones (in the case of the SA condition) convolved with the canonical hemodynamic response function (HRF) as implemented in the SPM (Statistical Parametric Mapping) software toolbox [29].

3.3 Preprocessing

The data must undergo several preprocessing steps before being analyzed or used for classification. The preprocessing steps are similar when working with both datasets. First, the images are converted from DICOM to NIFTI format using the dcm2niix tool [30]. Then, a bias field correction is applied, followed by functional realignment and unwarping, slice-timing

correction, direct segmentation and normalization, and smoothing. This pipeline is labeled as the 'default preprocessing pipeline for volume-based analyses (direct normalization to MNI-space)' in the CONN toolbox [31]. The preprocessed data were provided by the diploma thesis consultant Ing. David Tomeček.

The dataset is further analyzed to check whether all subjects' volumes are in the field of view (FOV) – the area that is imaged during scanning – and are sufficiently covered. An overlap of each subject's FOV and regions of the Automated Anatomical Labeling (ALL) atlas [32] is computed and then used as a criterion for selection. The number of regions that are less than 50% covered is computed. The selection criterion is subsequently set so that subjects with the number of uncovered regions above the 95th percentile are discarded.

3.4 Analyses

3.4.1 Independent component analysis

Independent component analysis (ICA) is computed to find the key functional brain networks responsible for self and other-agency judgment. It is performed using the Group ICA (GIFT) toolbox by Calhoun et al. [33], [34]. In the case of this study, the independent components are found with the approach of minimizing mutual information, the Infomax algorithm described in Section 2.2.2. The number of required estimated independent components was set to 35, according to the study by Spaniel et al. [3].

As a part of the replication study, the ICA is evaluated three times. Once on the IKEM dataset, once on the independent NIHM dataset, and once on the merged IKEM and NIHM datasets. The resulting *beta weights* of IKEM and merged dataset analyses are further used to classify FES and HC.

ICASSO To obtain a more reliable estimate of the independent components, ICA is repeated for each subject twenty times – with different initial values and differently bootstrapped datasets. The best result is chosen from the twenty runs of ICA and considered the independent component. This method is called ICASSO [17], and it is a part of the GIFT toolbox

[33], [34].

ICASSO provides an insight into the components' stability. Based on standard procedures [17], components with a stability index larger than 0.9 are considered reliable, but the rest are excluded from further analysis.

Selection of relevant components To determine which of the estimated components are essential in the context of the Self-agency experiment, I set several conditions that must be met. First, the components should be reliable in terms of ICASSO. Second, there has to be a substantial correlation ($|r| > 0.5$) between the time course of the experiment and the mean component time course component across patients. And third, there must be a significant difference between the FES and HC groups in that component's activity. To explore the last criterion, a two-sample t-test is evaluated. The level of significance is set to $\alpha = 0.05$. (The two-sample t-test is not applied when the components are selected as features for the classification task.)

Additionally, there is a visual check of mean independent components. According to [11], components are assessed and eventually marked as artifacts. Components identified as artifacts are excluded from further evaluation.

3.4.2 Voxel-wise analysis

Statistical Parametric Mapping (SPM) was chosen as the analysis of the Self-agency experiment data, according to [3]. The analysis is performed using the SPM12 toolbox [29]. It is performed twice, once on the IKEM dataset and once on the independent NIHM dataset. The *beta weights* obtained from the IKEM dataset are then learned by the classifier, which is then used for the classification of the NIHM data.

First, the general linear model is fit to the time course of the brain activity at each voxel, according to the equation 8. As described in Section 2.3, the design matrix includes condition-specific effects but also confounding effects and constant term. Following the chosen approach of one time series describing the course of the experiment, and to simplify for further expla-

nations, there is, in principle, one regressor, and the equation simplifies to:

$$Y = \beta_0 + \beta_1 X_1 + \epsilon, \tag{18}$$

where Y is the vector whose individual elements correspond to individual activity measurements in time, and X_1 is the time course of the experiment. β_0 and β_1 are coefficients, β_1 is hereafter referenced as *beta weight*. Regressor X_1 was generated by the convolution:

$$X_1 = C * f, \tag{19}$$

where C is an alternating sequence of blocks of zeros and ones corresponding to the design of the experiment - sequences of zeros representing the first condition (OA) and sequences of ones representing the second condition (SA); f is the canonical hemodynamic response function (HRF). The number of zeros/ones at each series corresponds to the number of scans during that experiment block.

After the model estimation, SPM provides an analysis mask image for each subject. It is an image of zeros and ones indicating which voxels were included in the analysis. When generated implicitly, the mask is based on excluding voxels with intensity below a certain threshold, which is used to exclude artifacts caused by motion or noise. All masks are visually checked and if a substantial visible uncovered area exists, the subject is excluded from the dataset. Note that this is an additional quality control step on top of removing subjects with too many regions with less than 50% coverage as described in Section 3.3.

Then, the data undergo the group analysis (second-level analysis in the SPM terminology). In this case, the one-sample t-test is computed separately for both groups – FES and HC – to test whether the mean activation of each voxel in the group is significant. A two-sample t-test is also calculated to see if there is a significant difference between the two groups.

3.5 Feature selection

In this section, I describe the methods of feature selection used for the classification task. In both classification tasks, whether performed on the results of ICA or the results of voxel-wise analysis, classification is based on utilizing the *beta weights* β_1 obtained from the initial analysis. In both cases, β_1 are coefficients in the simplified general linear model:

$$Y = \beta_0 + \beta_1 X_1 + \epsilon, \tag{20}$$

where X_1 stands for the time course of the experiment. Y is a time course of BOLD signal in a particular region that is given by the analysis type.

3.5.1 ICA

In the context of the ICA results, GLM is fit to the activity course (time series) of each component. In equation 20, Y is the time course of the independent component, X_1 is the time course of the experiment. In summary, we get a matrix of *beta weights* **B** of size *[number of subjects, number of components]*.

Feature selection then depends on the previous examination of estimated independent components, described in 3.4.1. Components found to be reliable by the ICASSO method, significantly correlated with the experiment's time course, and not labeled as artifacts are selected as features for the classification task. The two-sample t-test is not applied in the case of feature selection for the classification task to prevent data leakage.

3.5.2 Voxel-wise analysis

In the case of voxel-wise analysis, I get the 3D matrix of *beta weights* **B** directly from the SPM procedure, as described in Section 3.4.2. However, **B** is a three-dimensional matrix of size [109, 91, 109] for each subject, and it is necessary to effectively reduce its size so that I can use it as a matrix of features for the classifier.

Before any dimensionality reduction, it is useful to check whether the masks created during SPM sufficiently cover the volume of the brain. Non-covered areas of the brain may appear in the mask and then propagate to **B** as a not-a-number value. The coverage is checked visually by displaying the subjects' SPM masks as described in Section 3.4.2.

Clustering As for dimensionality reduction, I decided to approach it via clustering and projection to low-dimensional space. I chose simple linear iterative clustering (SLIC) [19] as a clustering method.

First, I create a mask $\mathbf{M_0}$, that is equal to *0* at every voxel, which was not-a-number for any of the subjects, and that is equal to *1* otherwise. Every data point is multiplied with this mask; let's denote the result containing all subjects as $\mathbf{B_0}$. Then, I construct a similar mask, except that instead of zeros, the not-a-number values are replaced with number *10*, since it is a significantly larger value than the values of *beta weights*. Let's denote the mask as $\mathbf{M_L}$ and the result of its multiplication with the data as $\mathbf{B_L}$.

$\mathbf{B_L}$ is then split into two matrices, one containing only the data of HC and one only the data of FES patients. Each matrix is then averaged along subjects, and we get $\mathbf{B_{L,HC}}$ and $\mathbf{B_{L,FES}}$. $\mathbf{B_{L,HC}}$ and $\mathbf{B_{L,FES}}$ are concatenated to form a matrix $\mathbf{B_{L,avgs}}$ of shape *[x, y, z, 2]*.

Next, $\mathbf{B_{L,avgs}}$ is used as an input to SLIC. As described in detail in Section 2.4, this method performs k-means clustering restricted to parts of the image and, using the information of image channels, prefers clustering pixels with the same color (channel values). In this case, $\mathbf{B_{L,HC}}$ and $\mathbf{B_{L,FES}}$ serve as two channels of an image $\mathbf{B_{L,avgs}}$.

SLIC requires filling several parameters that determine the clustering result: *number of superpixels* (approximate number of clusters), *compactness* (a parameter that balances color proximity and space proximity), and *enforce of connectivity* parameter (determines, whether the generated superpixels are connected or not). The number of superpixels is set to 500 based on my previous experience with this algorithm when applied to MRI images. The same applies to the compactness parameter, which was set to 0.2 since lower values (default = 10) give more weight to color proximity. Enforce connectivity parameter was set to *True*.

Once found, clusters are applied to each subject in $\mathbf{B_0}$. Then, the mean across all corresponding *voxel beta weights* is calculated in each superpixel.

Partial least squares The number of potential features was reduced with SLIC to approximately 500. Since the dataset size is much smaller and I aim to have a low-dimensional model, the number of features must be further reduced.

A way to reduce the number of features is by transforming superpixels' means into a low-dimensional space. In this particular case, it is useful to reach for a transformation that will, besides explaining the maximum variance, preserve differences between groups. This can be

achieved by the Partial Least Squares method (PLS), described in more detail in Section 2.5.

The only parameter to be set is the number of features to which one wants to reduce the data. The number of features optimization is described in the next paragraph.

Optimal number of features The optimal number of features for the classification task based on the *beta weights* obtained from the voxel-wise analysis (described in detail in Section 3.5.3) is searched by repeating the leave-one-out cross-validation process on the IKEM dataset for the number of features $f \in [1, 2, 4, 6, \ldots, 60]$. Note that the search is performed on the whole IKEM dataset, which introduces a risk of overfitting. Thus, a further described classification of the independent dataset is performed for several options of the number of features. Since I aim for a low-dimensional model, one of the options of this hyperparameter is given by a local maxima of accuracy for the number of features below $f \leq 20$, if there is any.

3.5.3 Classification

The comparison of tested methods is approached by comparing the performance of a classifier, once trained and tested on the *beta weights* obtained from ICA, once on the *beta weights* obtained from the voxel-wise analysis.

Support vector machine with linear kernel was selected as the classifier. To get an idea of its performance, it is trained and validated within leave-one-out cross-validation on the whole dataset. In particular, in the leave-one-out cross-validation, the dataset is divided into training and validation parts, where the validation part consists of a single data point (subject), and the validation part consists of the rest of the dataset. Before the features enter the classifier, their values are normalized with z-score normalization.

3.5.4 Compensating for imbalanced dataset

Since the representation of FES and HC classes in the dataset is not balanced, weights are pre-computed to compensate for this problem and to ensure that learning is not biased. The weights enter the classifier during the training process and are used in the classifier's perfor-

mance measurement. The weights assigned to the data from one class w_{class} are computed in the following way:

$$w_{class} = \frac{1}{2} \cdot \frac{s_{all}}{s_{class}}, \tag{21}$$

where s_{class} is the number of subjects in the class, and s_{all} is the number of all subjects (subjects in both classes).

3.5.5 ICA

The classification into FES and HC classes for the independent component analysis outputs is based on the *beta weights* corresponding to the selected independent components. These values enter the classifier as a set of features. The whole process of the classification based on ICA *beta weights* is carried out within the leave-one-out cross-validation.

3.5.6 Voxel-wise analysis

When the classification is based on the results of voxel-wise analysis, the only part of the process that is outside the leave-one-out cross-validation loop is the loading of the data and masking it to get $\mathbf{B_0}$ and $\mathbf{B_L}$ as described in the Section 3.5.2.

Then, the data in the form of matrices $\mathbf{B_0}$, $\mathbf{B_L}$ are split into training and validation parts. On training data, clustering with the SLIC superpixels method is computed, and the PLS transformation is found. Both are then applied to the validation part of the data. Afterward, training and validation sets with the desired number of features are fed to the classifier.

3.6 Regression

The regression task was set to predict values of the PANSS scale using the same features as for classification. It is focused on predicting PANSS values that summarize different categories of symptoms: positive, negative, general, and total summary of all symptoms.

The prediction procedure was very similar to the classification task. In the case of ICA, features are *beta weights* of selected independent components. In the case of voxel-wise ana-

lysis, there is the very same process of dimensionality reduction of *beta weights*, as described in Section 3.5.2. In both cases, the dataset is weighted to compensate for its imbalance, and the data are normalized.

As a model, support vector regression was chosen. It was tested with linear kernel, radial basis function kernel, and polynomial kernel. The regression is performed within the leave-one-out cross-validation to get an insight into the model performance.

4 Results

4.1 Replication study

The replication study was conducted on two separate datasets – the IKEM dataset and the NIHM dataset (see Section 3.1). As the first part of the replication study, I preprocessed the data from both datasets and checked the brain volume coverage of each subject. In the case of the IKEM dataset, this step excluded 5 subjects who were outside the 95th percentile of the number of under-covered brain regions. A histogram showing the distribution of the number of under-covered areas for each subject is shown in Figure 7.

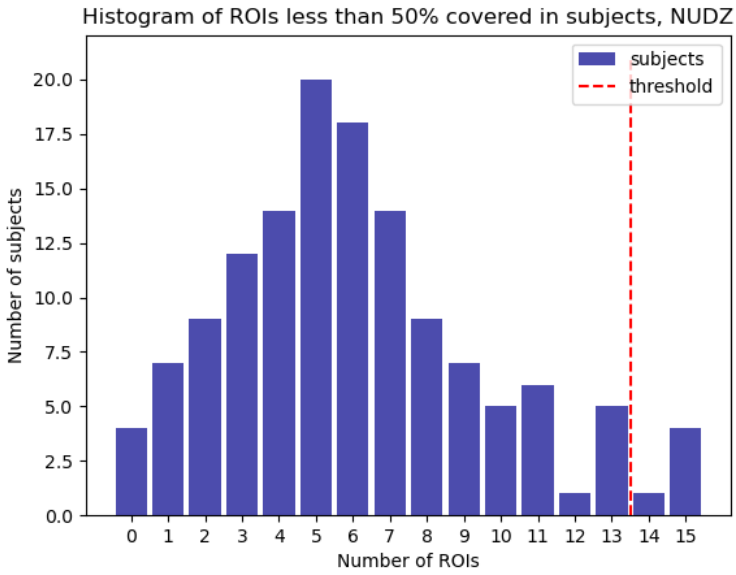

Figure 7: Histogram of the number of brain areas that were less than 50% covered in subjects from the IKEM dataset. Above the exact threshold of the 95th percentile would be the top seven subjects, but since a precise threshold in the number of under-covered areas was required, the threshold was moved to the nearest whole number of under-covered areas, i.e., 14, and the top 5 subjects were excluded.

In the case of the dataset obtained from NIHM, from the original dataset of size 165 subjects, seven subjects were excluded, and the dataset further consisted of 158 subjects – 66 HC and 92 FES patients. A histogram of the number of under-covered areas for each subject is shown in Figure 8.

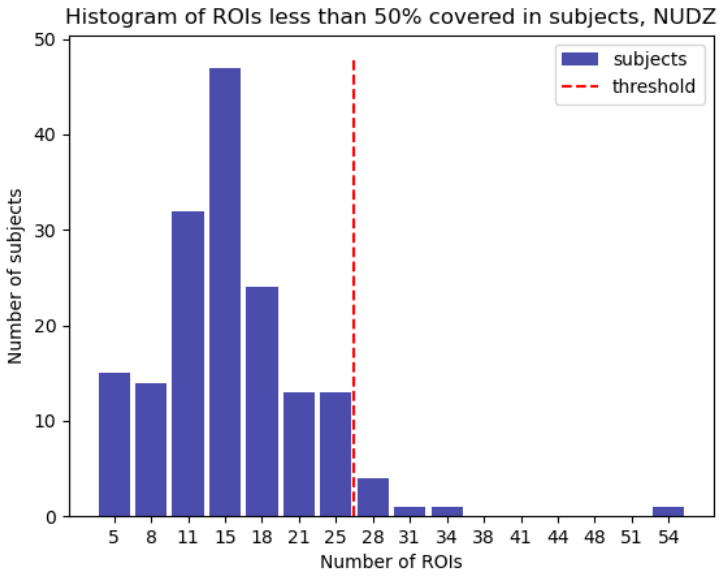

Figure 8: Histogram of the number of brain areas that were less than 50% covered in subjects from the NIHM dataset. Above the exact threshold of the 95th percentile would be the top 8 subjects, but since a precise threshold in the number of under-covered areas was required, the threshold was moved to the nearest whole number of under-covered areas, i.e., 26, which excluded the top 7 subjects.

4.1.1 ICA of the IKEM dataset

On the remaining subjects from the IKEM dataset, exactly 131, group independent component analysis was computed. The ICA was run 20 times following the ICASSO method. ICA was used to extract 35 independent components.

The selection of relevant components identified the following: ICASSO excluded one com-

ponent with a stability index below 0.9. A substantial correlation ($|r| > 0.5$) between the time course of the experiment (convolved with the canonical hemodynamic response kernel) and the mean (across subjects) activity of the component was present in 11 components - 6 with positive correlation and 5 with negative. According to the two-sample t-test, 2 of the remaining components were not significantly different in the HC and FES groups. The two components are not considered when evaluating the results of the analysis but are included in the classification task. Finally, a visual evaluation of results identified one artifact among the significant components that was also subsequently excluded. The results of the relevant components selection can be found in Table 25 in the Appendix.

In Figure 9 are depicted the components that were positively correlated with the time course of the experiment. On the other side, the negatively correlated components are shown in Figure 10. All selected components are listed in Table 3.

C no.	**r**	**brain area**	**function**
5	+	visual cortex	processes visual information
10	+	artifact	-
20	+	visual cortex	processes visual information
22	+	middle frontal gyrus	cognitive control, language, motoric
24	+	inferior parietal lobule	cognition and somatosensory processes
31	+	superior frontal gyrus	cognitive control, self-awareness, motor planning
7	-	medial prefrontal cortex, ACC	self-identity, social cognition
15	-	precuneus, parietal lobe, ACC	self-awareness, self-reflection
16	-	primary auditory cortex	processing of auditory information
19	-	precuneal and cuneal cortex	self-awareness, self-reflection, visuospatial p.
30	-	precuneus	self-awareness, self-reflection

Table 3: Table of relevant components estimated from the IKEM dataset, including their identification number (C no.), that were positively (+) or negatively (-) correlated with the time course of the experiment, their localization, and likely function. (ACC stands for the anterior cingulate cortex.)

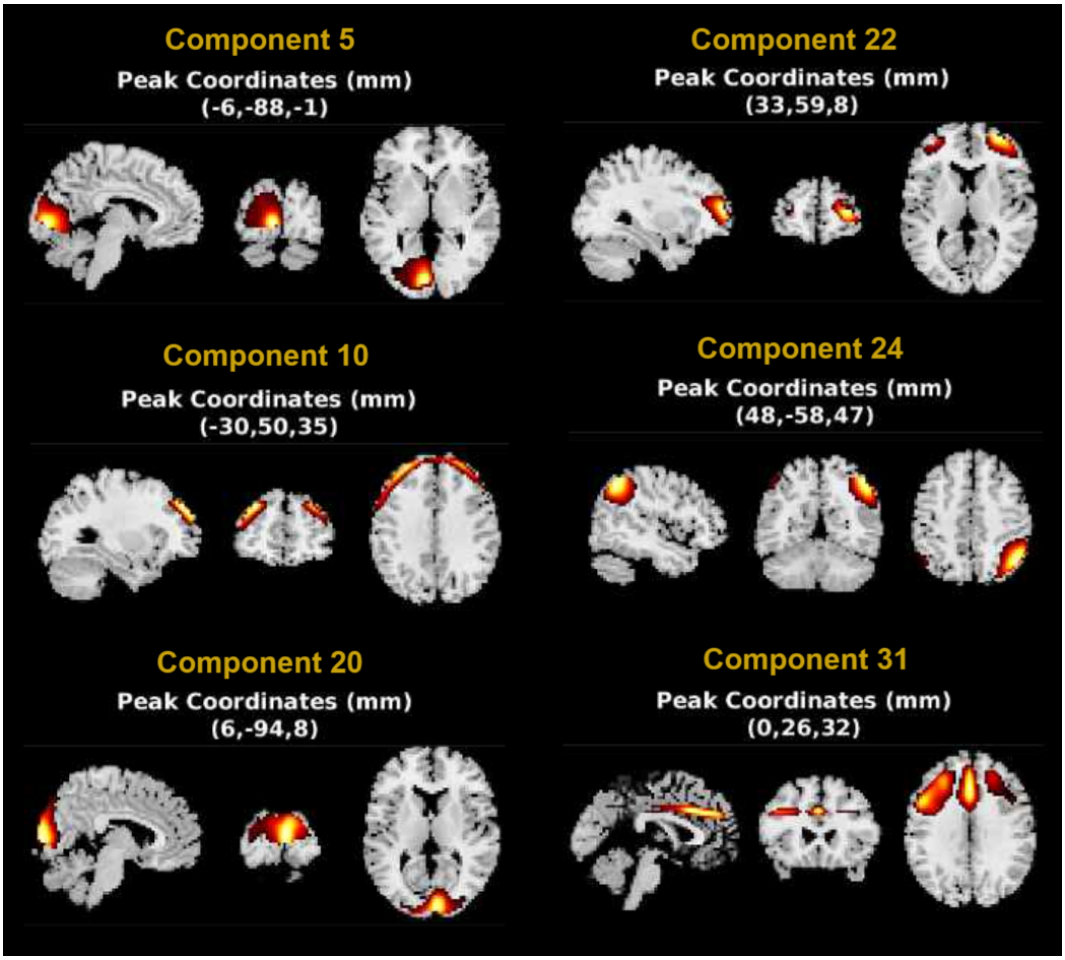

Figure 9: Components estimated from the IKEM dataset, positively correlated with the time course of the experiment, displayed in the axial, sagittal, and transversal planes. The component loadings are thresholded at $z > 3$ for easier visual localization of most involved brain regions. See Table 3 for more details.

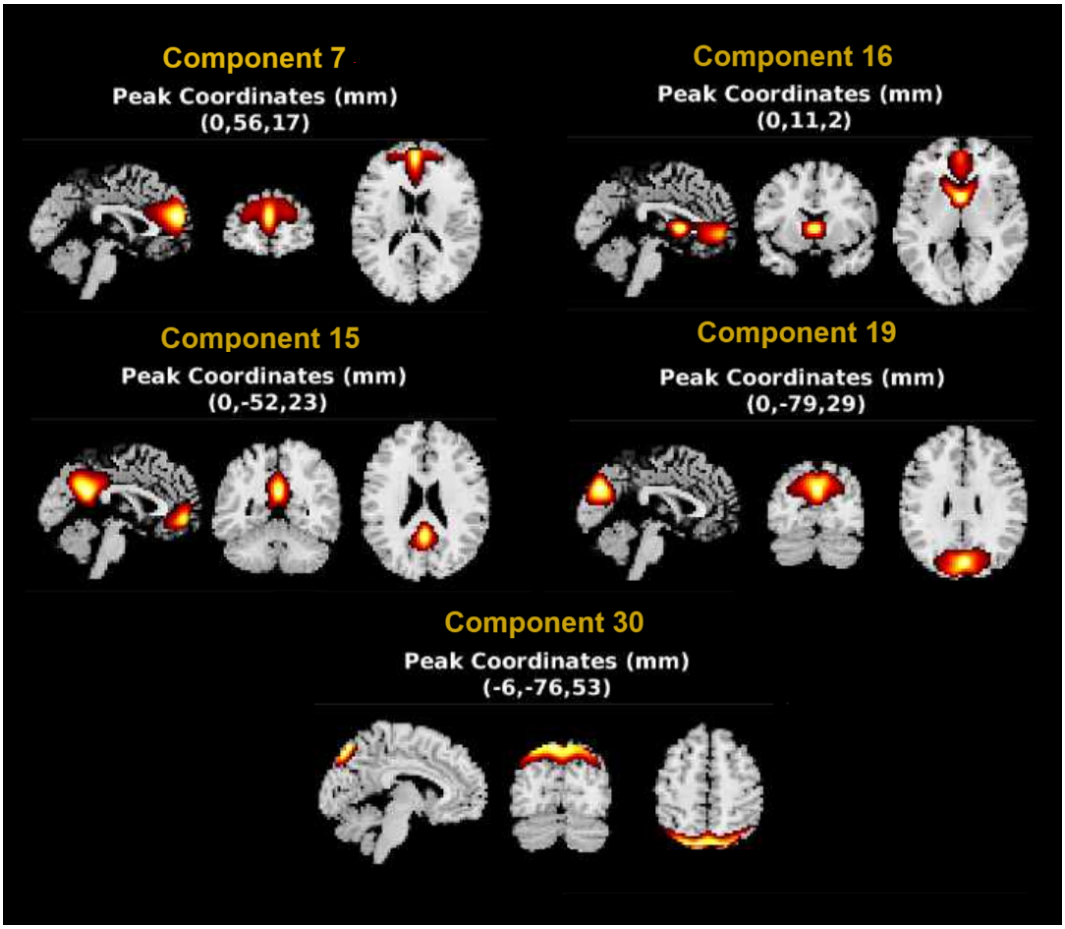

Figure 10: Components estimated from the IKEM dataset, negatively correlated with the time course of the experiment, displayed in the axial, sagittal, and transversal planes. The component loadings are thresholded at $z > 3$ for easier visual localization of most involved brain regions. See Table 3 for more details.

4.1.2 ICA of the NIHM dataset

Independent component analysis was computed on the NIHM dataset. Same as in the previous case, the ICA was run 20 times following the ICASSO approach, and 35 components were estimated. Components with a stability index below 0.9 were categorized as unstable based on the standard ICASSO convention [17] and excluded from further processes.

The selection of significant components resulted in the following: A substantial correlation ($|r| > 0.5$) was found in 9 components – 4 showed a positive correlation with the time course of the experiment, 5 showed a negative correlation. An additional two-sample t-test excluded 2 other estimated components since there was not a significant difference between HC and FES groups in these components. A visual evaluation revealed 2 artifacts among the significant estimated components. The overall results of the selection are shown in Figure 25 in the Appendix.

Relevant components were identified according to Section 3.4.1 and are listed in Table 4. Figure 12 shows components positively correlated with the time course of the experiment. Figure 11 shows negatively correlated components.

C no.	**r**	**brain area**	**function**
20	+	artifact	-
22	+	sec. somatosensory cortex	somatosensory processes
23	+	sec. somatosensory cortex (right)	somatosensory processes
30	+	superior parietal lobule	visuospatial processes
2	-	cuneal cortex	visual processing
3	-	somatosensory and motor cortex	somatosensory processes, motoric
5	-	artifact	-
12	-	precuneal cortex, ACC	self-awareness, self-reflection
18	-	medial prefrontal cortex, ACC	self-identity, social cognition

Table 4: Table of significant components (C no.) estimated on the NIHM dataset that were positively (+) or negatively (-) correlated with the time course of the experiment, their identification, and function.

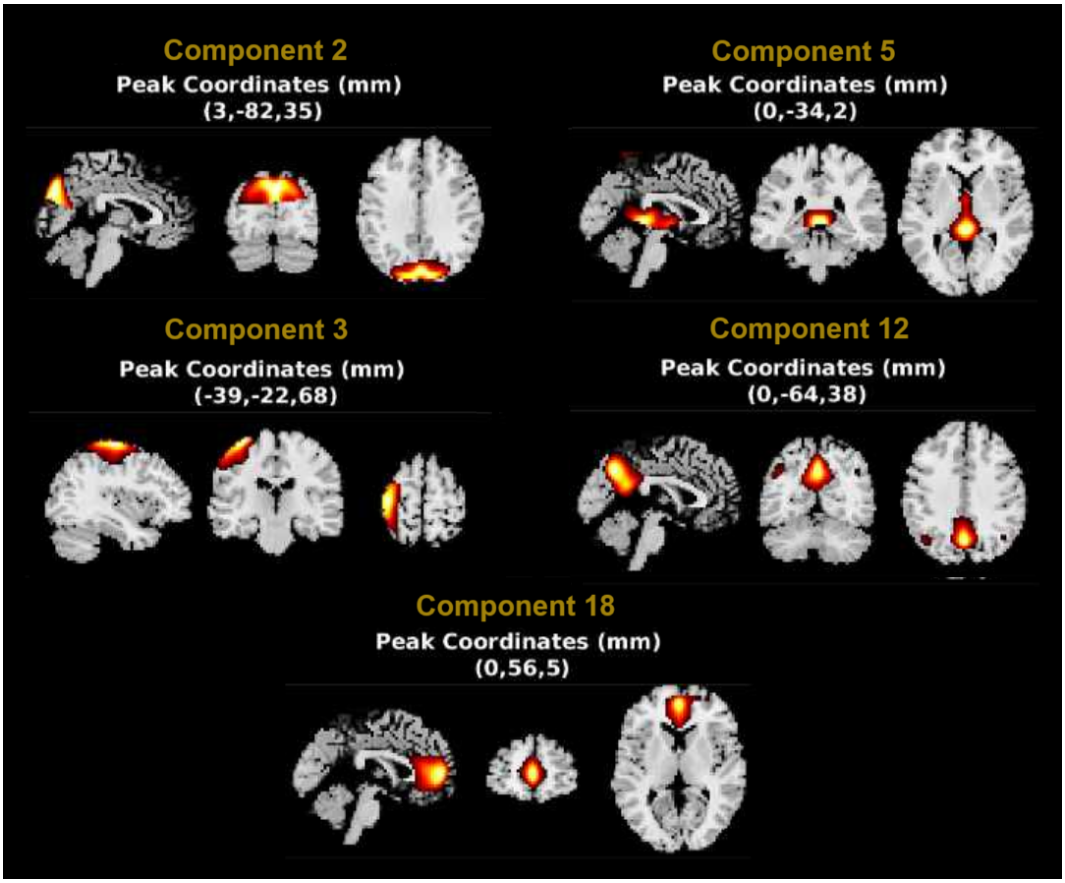

Figure 11: Components estimated from the NIHM dataset, negatively correlated with the time course of the experiment, displayed in the axial, sagittal, and transversal planes. The component loading are thresholded at $z > 3$. See Table 4 for details.

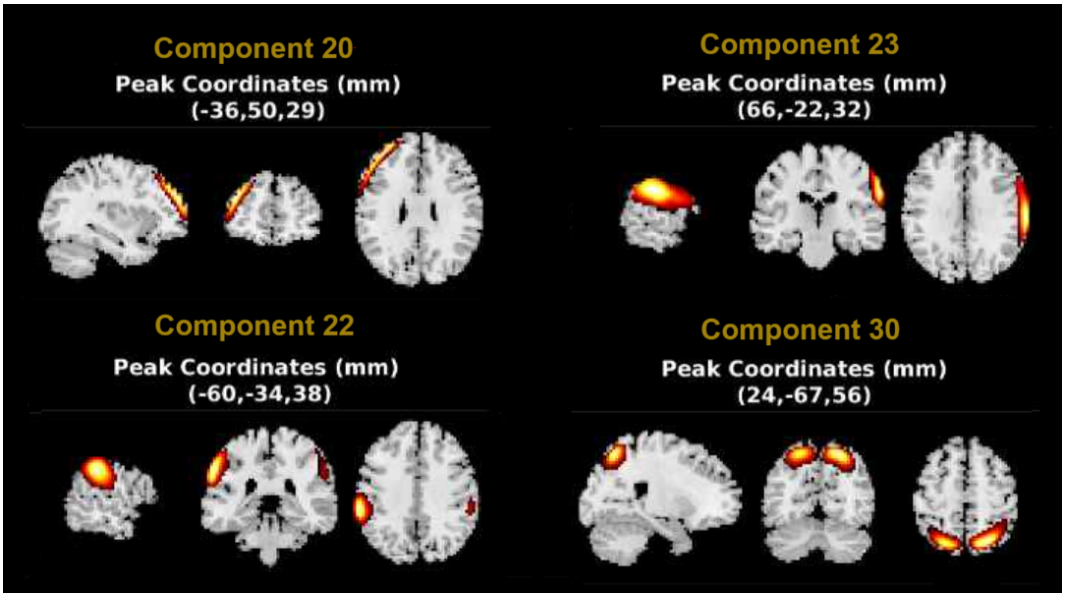

Figure 12: Components estimated from the NIHM dataset, positively correlated with the time course of the experiment, displayed in the axial, sagittal, and transversal planes. The component loadings are thresholded at $z > 3$ for easier visual localization of most involved brain regions. See Table 4 for more details.

4.1.3 ICA of merged IKEM and NIHM datasets

For the purposes of the classification task, ICA was also computed for merged IKEM and NIHM datasets. The selection of significant components resulted in the following: A significant correlation ($|r| > 0.5$) was found in 13 components – 6 showed a positive correlation with the time course of the experiment, 7 showed a negative correlation. An additional two-sample t-test excluded 2 other estimated components since there was not a significant difference between HC and FES groups in these components. A visual evaluation revealed 2 artifacts among the significant estimated components. The overall results of the selection can be found in Table 25 in the Appendix.

Relevant components were again identified according to ref. Figure 13 shows components positively correlated with the time course of the experiment. Figure 14 shows negatively

correlated components. All relevant components are listed in Table 5.

C no.	**r**	**brain area**	**function**
8	+	middle frontal gyrus (left)	cognitive control, language, motoric
16	+	artifact	-
18	+	V5, middle temporal gyrus	auditory and visual processes, language
20	+	superior frontal gyrus	cognitive control, self-awareness, motor planning
22	+	middle frontal gyrus (right)	cognitive control, language, motoric
34	+	inferior parietal lobule	cognition and somatosensory processes
5	-	medial prefrontal cortex, ACC	self-identity, social cognition
6	-	cuneal cortex	visuospatial processes
17	-	precuneus, V5	self-reflection; visual processes
21	-	primary auditory cortex	processes auditory information
26	-	precuneus, parietal lobe	self-awareness, self-reflection
30	-	artifact	-
31	-	visual cortex	processes visual information

Table 5: Table of significant components (C no.) estimated on merged IKEM and NIHM datasets that were positively (+) or negatively (-) correlated with the time course of the experiment, their identification, and function.

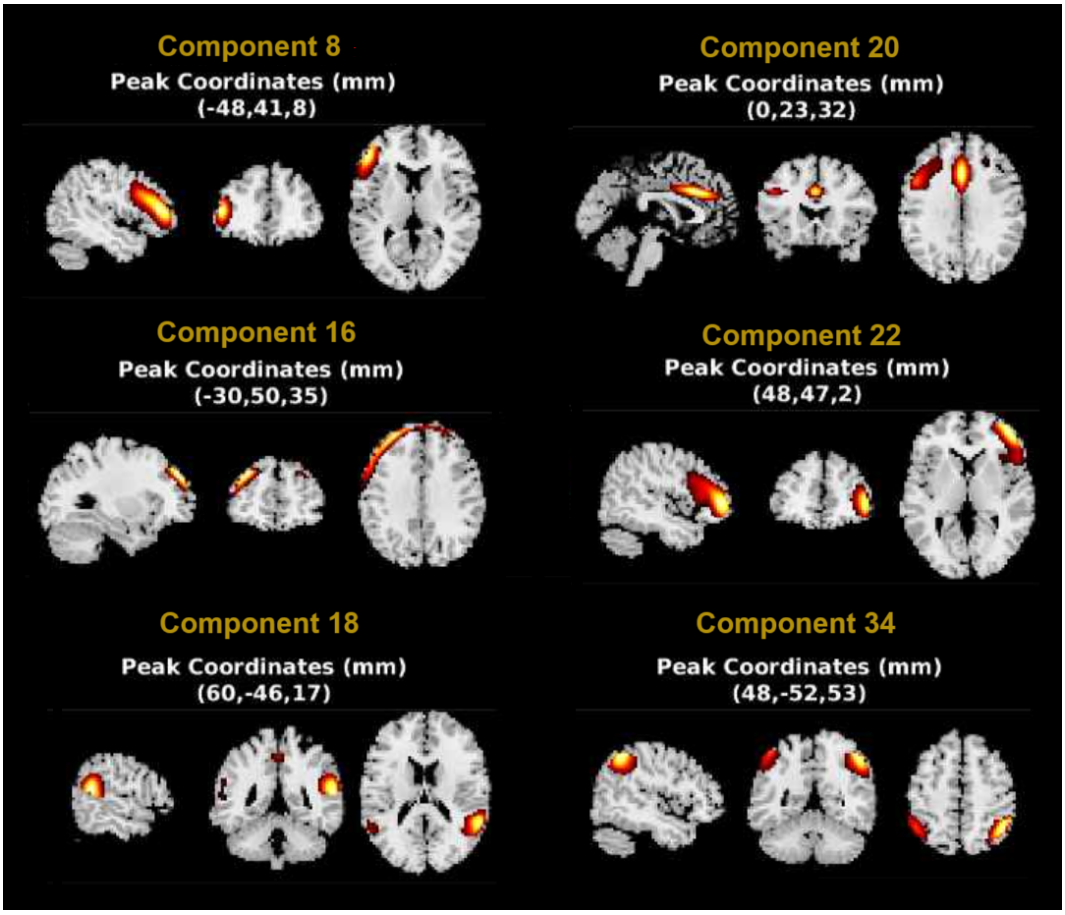

Figure 13: Components estimated from the merged IKEM and NIHM datasets, positively correlated with the time course of the experiment, displayed in the axial, sagittal, and transversal planes. The component loading are thresholded at $z > 3$ for easier visual localization of most involved brain regions. See Table 5 for more details.

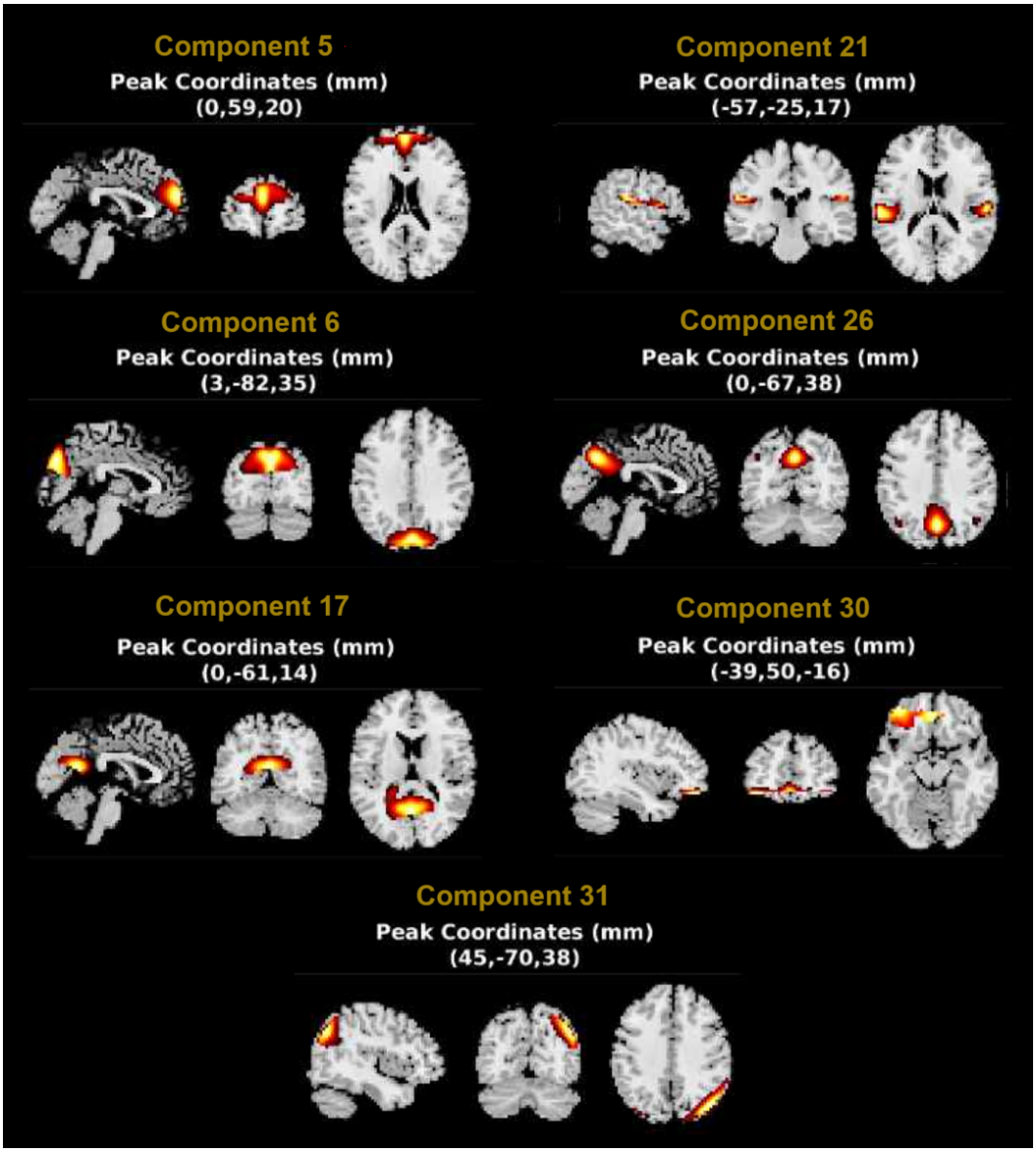

Figure 14: Components estimated from the merged IKEM and NIHM datasets, negatively correlated with the time course of the experiment, displayed in the axial, sagittal, and transversal planes. The component loadings are thresholded at $z > 3$ for easier visual localization of most involved brain regions. More details are listed in Table 5.

4.1.4 Voxel-wise analysis of the IKEM dataset

According to the previous study, as a second commonly used analysis, voxel-wise analysis obtained from statistical parametric mapping was evaluated. The general linear model was fit to the brain activity time course in each voxel for each subject, using the SPM12 toolbox. This yielded *beta weights* that are later used for classification in Section 4.3 in this Chapter. In addition to checking brain coverage within the FOV as described above and shown in Figure 7, the masks created during the SPM analysis were checked to exclude subjects with potentially undercovered brain volumes due to motion artifacts. Following this check, one FES patient was removed; the mask is displayed in Figure 15.

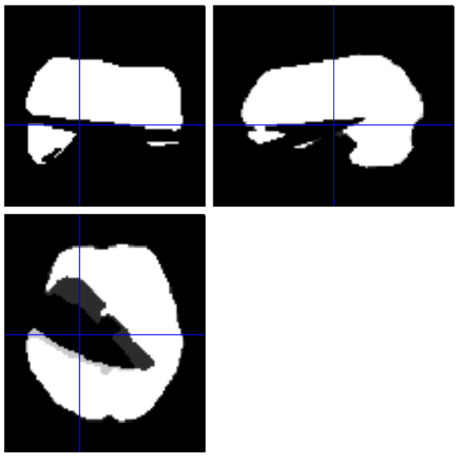

Figure 15: SPM-generated mask of the subject that was excluded due to a substantial uncovered area of the brain, which was probably caused by the subject's movement.

In addition, statistical tests were performed to determine: first, which voxels were statistically significantly active in each group (HC, FES) during each condition (OA, SA) and then whether there was any difference between the HC and FES groups during either OA or SA condition.

Group analysis A one-sample t-test was evaluated in every voxel to determine whether the mean activation was significantly stronger during OA compared to SA and vice versa for

FES and HC groups. It was computed separately for each group and for each condition. The t-maps are shown in Figure 16.

The FES group exhibited strong increased activity in the visual cortex and anterior insula during the OA blocks compared to the SA blocks of the experiment. During the SA blocks, there was an increased activation in the visual cortex and anterior DMN area in comparison to OA blocks.

HC showed extended activity, especially in the dorsal lateral prefrontal cortex, during the OA condition when compared to the SA condition. During the SA condition, there was a prominent activity in the areas of anterior and posterior DMN in comparison to the OA condition.

Group comparison A two-sample t-test was evaluated to determine whether there was a significant difference between the group of HC and the group of FES patients during the Self-agency experiment. The test showed a marked difference between the two groups: HC exhibited extended activation in the region of the premotor cortex during OA when compared to the SA condition. During SA, there was a stronger activation in the case of HC than FES in the anterior and posterior parts of the DMN in comparison to the OA condition. This applies to FES the other way around. FES had a stronger activation than HC in the anterior and posterior DMN during OA compared to SA blocks; during SA blocks, there was a marked activation in the premotor cortex in comparison to OA blocks.

4.1.5 Voxel-wise analysis of the NIHM dataset

Voxel-wise analysis was computed for the NIHM dataset, too. The general linear model was fit to the data using the SPM12 toolbox. Next, the masks created during the analysis were checked to exclude potential undercovered brain volumes. In this case, none of the subjects was removed.

Obtained coefficients – *beta weights* – underwent a statistical test to determine significant activities in each group (HC, FES) during each condition (OA, SA) and also any potential differences between the groups during each condition.

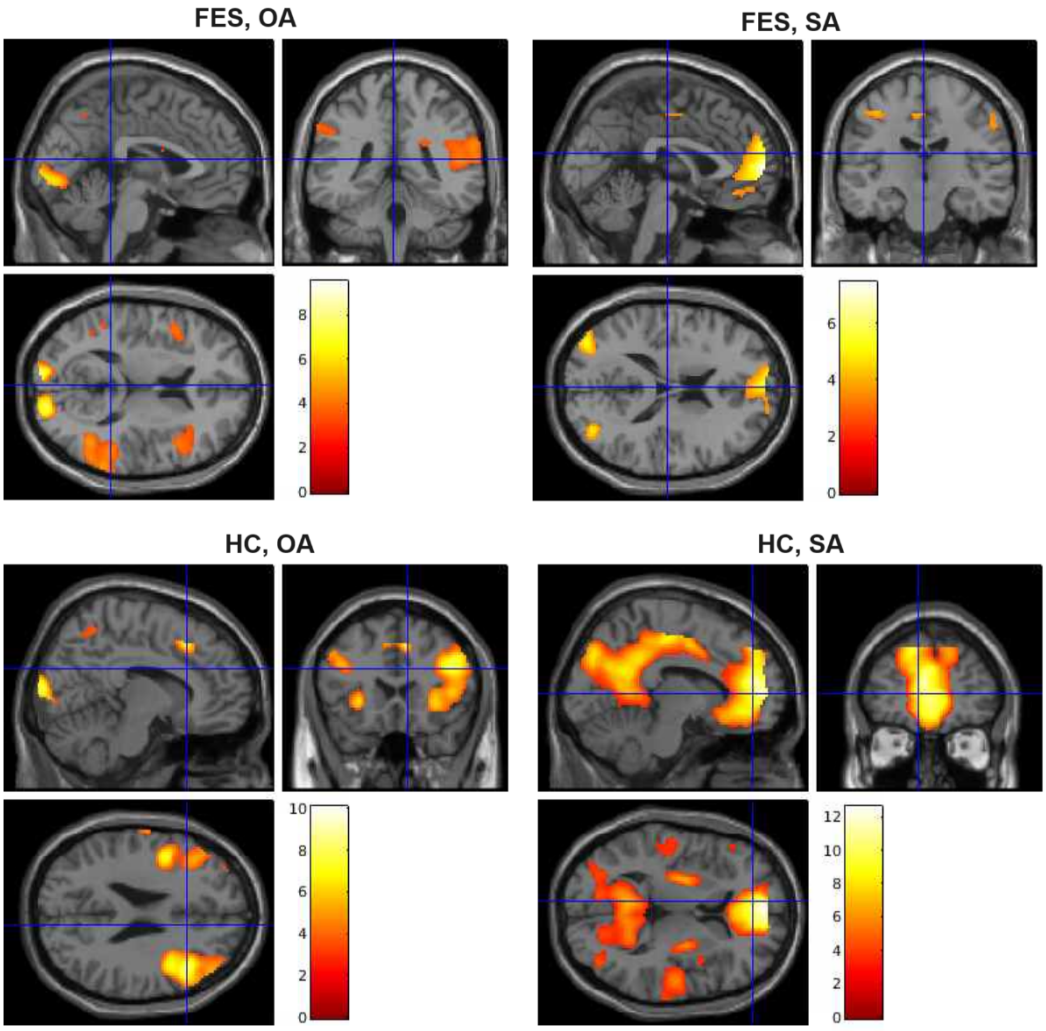

Figure 16: Results of one sample t-test (FWE corrected, voxel level, $P < 0.05$) showed as colormaps on MNI template in the axial, sagittal, and transversal plane for the IKEM dataset. The test was computed for both groups (FES and HC) and both conditions (OA and SA). The FES group exhibited the stronger activity in the visual cortex during the OA condition than SA condition and in anterior DMN during the SA condition more than the OA condition. HC showed significant activation in the dorsal lateral prefrontal cortex during the OA condition in comparison to the SA condition and in the anterior and posterior parts of DMN during the SA condition more than during OA.

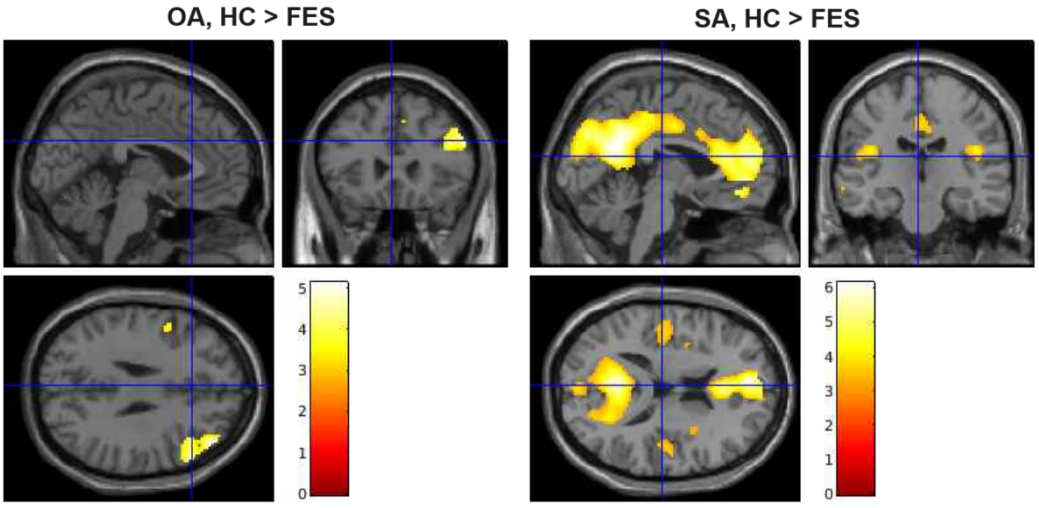

Figure 17: Results of two-sample t-test displayed as colormaps on MNI template in the axial, sagittal, and transversal plane for the IKEM dataset. The results show that the HC group exhibited stronger activation more than FES during the OA condition rather than the SA condition. During the SA condition, the area of anterior and posterior DMN exhibited stronger activation than during the OA condition.

Group analysis One-sample t-test was computed on *beta weights* to answer whether the mean activation is significantly greater than zero at any voxel. The test was calculated for each group and each condition separately, FWE was corrected on voxel level, $P < 0.05$.

The FES group exhibited marked activity in the anterior insula during the OA condition when compared to the SA condition. During the SA condition, there was stronger activity in the anterior and posterior parts of DMN and precuneus than during the OA condition.

HC showed activity in areas similar to the FES group, but the activation was much higher. During OA, there was activation in the somatosensory cortex more than during SA; the areas of anterior and posterior DMN were the most active during SA. Results are displayed in Figure 19.

Group comparison The group comparison was performed as a two-sample t-test separately for OA and SA conditions. The test revealed a great difference between FES and HC during SA condition when compared to the SA condition, especially in posterior and anterior DMN, where the HC group showed higher activations. During the OA condition, when compared to SA, there was almost no significantly higher activation in the HC group than in the FES group. Results of the two-sample t-test are shown in Figure 18.

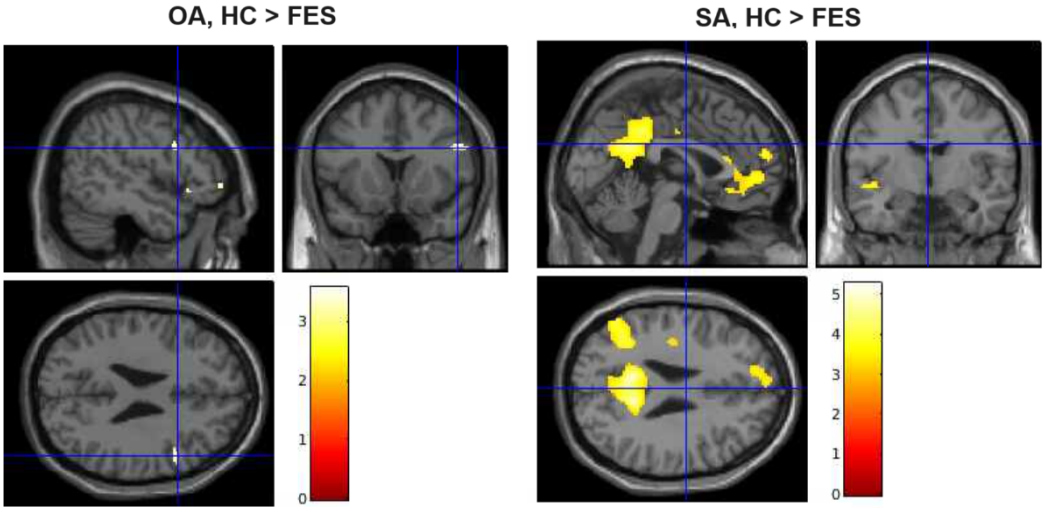

Figure 18: Results of two-sample t-test computed on NIHM dataset, displayed as heat maps on MNI template in the axial, sagittal, and transversal plane. The results show that the HC group exhibited stronger anterior and posterior DMN activation during the SA condition than during the OA condition. During the OA condition, there was almost no greater activation more prominent than during the SA condition in HC more than in FES.

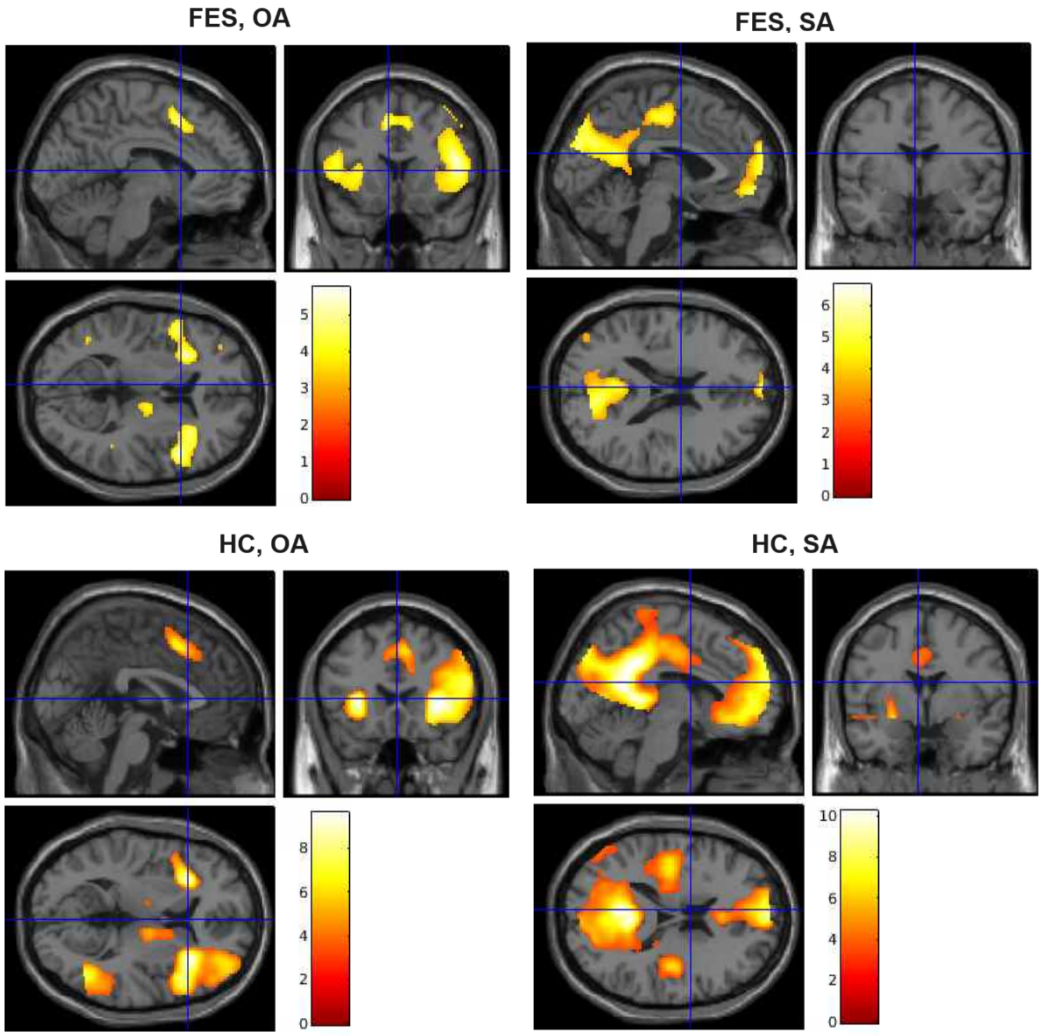

Figure 19: Results of one sample t-test computed on NIHM dataset, showed as heat maps on MNI template in the axial, sagittal, and transversal plane. The test was computed for both groups (FES and HC) and both conditions (OA and SA). The FES group exhibited significant activation in the somatosensory cortex during OA more than SA and anterior and posterior DMN during SA more than OA. The same applies to the HC group, except that the activations were of higher values.

4.2 Comparison of the ICA results

The independent component analyses showed that for the IKEM and NIHM datasets and subsequently for their combination, we obtained quite different results. When comparing the results of the IKEM and THE NIHM datasets, as matching components were identified, number 2 from IKEM and number 19 from NIHM, corresponding to the cuneal cortex; then numbers 12 and 18 from IKEM were similar to numbers 7 and 15 from NIHM that together comprise posterior and anterior parts of the DMN.

The ICA, which was additionally performed on the merged IKEM and NIHM datasets, revealed components:

- 5 corresponding to 7 from IKEM, labeled as the medial prefrontal cortex and ACC,
- 6 corresponding to 19 from IKEM, as precuneus and cuneus,
- 26 similar to 15, comprised of precuneus, parietal lobe, and ACC,
- 20 labeled as part of the superior frontal gyrus as number 31 from IKEM,
- 34 was similar to 24, as interior parietal lobule.

Since the difference between the two datasets was apparent already from the histograms 7 and 8, it is unsurprising that the analyses results differ. These results are further elaborated in the discussion 5.1.

4.3 Classification of the IKEM dataset

4.3.1 ICA

SVM classifier was chosen for the classification task. Its performance was evaluated based on the results of leave-one-out cross-validation executed on the whole dataset (131 subjects). The results are listed in Table 6; all values are computed with consideration of weights that

were pre-computed to compensate for the imbalanced representation of groups in the dataset. The receiver operating characteristic curve is displayed in Figure 20 to give a better idea of the classifier performance.

Accuracy (%)	78.16
Sensitivity (%)	76.32
Specificity (%)	80.00
AUC	0.85

Table 6: Performance of SVM classifier on the IKEM dataset, obtained from the results of leave-one-out cross-validation on the *beta weights* from ICA. The listed values were calculated with the consideration of weights.

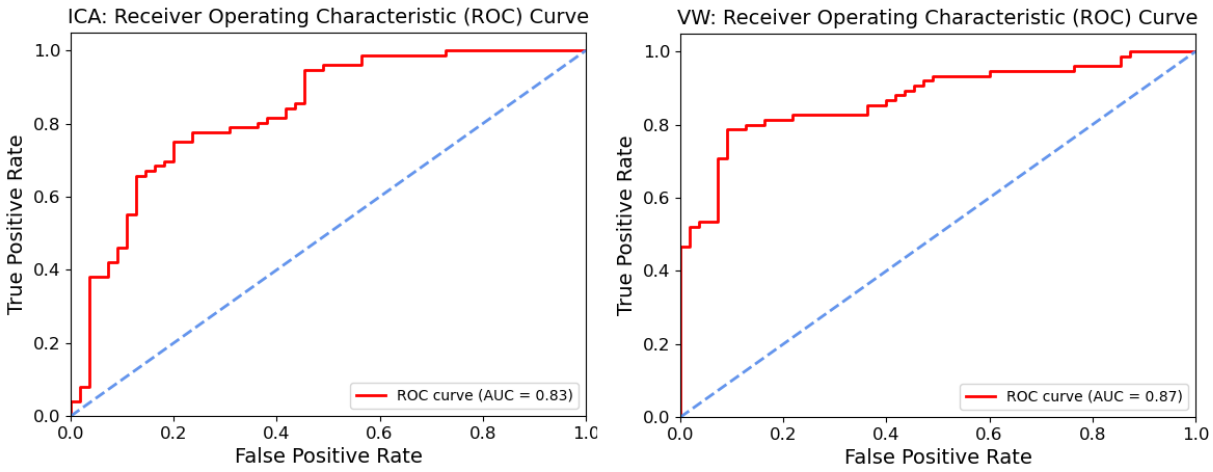

Figure 20: ROC curves obtained from leave-one-out cross-validation performed on the IKEM dataset. On the left, the result of the classification of ICA *beta weights*. On the right, the result of the classification based on the *beta weights* from the voxel-wise analysis.

4.3.2 Voxel-wise analysis

Classification based on voxel-wise analysis was conducted on 130 subjects – 55 HC and 75 FES patients. In this case, the classification can only be performed after dimensionality

reduction of *beta weights*, as described in section 5.2. The first step of the dimensionality reduction was to cluster the data with the SLIC algorithm. The result of clustering is shown in the form of several slices through the brain volume in Figure 24.

The optimal number of features was searched as described in Section 3.5.2. It was found that the function describing the dependence of the model accuracy on the number of features is rather noisy; see Figure 21. Therefore, the performance of the model is reported for several values of this hyperparameter. First, for the global optimum of the function in the interval [1, 20], i.e., 18 features, which was chosen since we were aiming for a low-dimensional model. Second, the global optimum of the function found at 48 and 52 features is reported. Lastly, the performance for 2 features is reported since the performance is already quite high for this very low number of features. After, partial least squares transformation was applied and produced the input for the classifier (for each of the mentioned number of features).

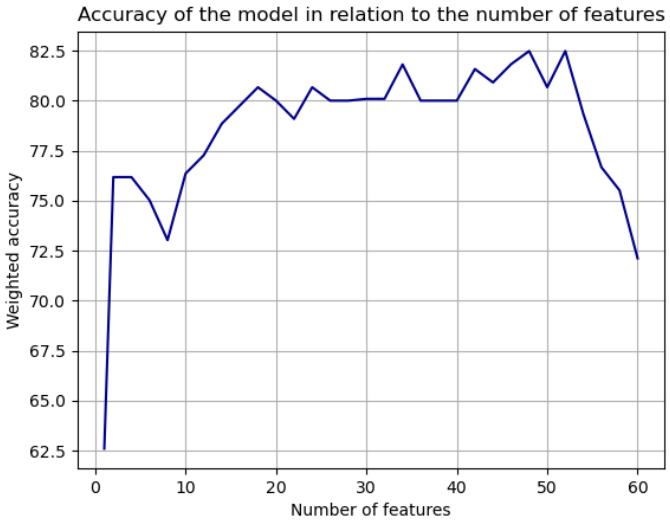

Figure 21: The weighted accuracy of the model in relation to the number of features. The stated accuracy was obtained from the leave-one-out cross-validation based on the *beta weights* from the voxel-wise analysis. The listed values were calculated with the consideration of weights.

f	2	18	48
Accuracy (%)	76.18	80.67	82.85
Sensitivity (%)	76.28	81.33	81.33
Specificity (%)	73.57	80.00	83.64
AUC	0.84	0.87	0.88

Table 7: Performance of SVM classifier on the IKEM dataset with a different number of features (f). The performance measures were obtained from the results of leave-one-out cross-validation on the features from the voxel-wise analysis.

SVM classifier with linear kernel was chosen for the classification task, as in the ICA-based classification. Its performance was evaluated based on the results of leave-one-out cross-validation executed on the whole dataset (130 subjects). The evaluation was run for the number of features $f = 2, 18, 48$. The results are listed in Table 7, all values are computed with consideration of weights that were pre-computed to compensate for the imbalanced representation of groups in the dataset. In Figure 20, the receiver operating characteristic curve is displayed to give a better idea of the classifier performance.

4.4 Classification of the NIHM dataset

The classification was performed using SVM with a linear kernel. I attempted to test the application of the already-trained classifier on an independent dataset. The actual process was that the SVM classifier was trained on the *beta weights* obtained from the IKEM dataset, and then subjects from the NIHM dataset were labeled by feeding the trained classifier with their *beta weights*.

4.4.1 ICA

Classification based on the results from ICA operated with the ICA components that were estimated for the merged IKEM and NIHM datasets (total of 289 subjects – 121 HC and 168 FES patients). The *beta weights* corresponding to the NIHM subjects are fed to the

classifier trained on the IKEM dataset. The classification results are listed in Table 8; all values include the consideration of weights that were pre-computed to compensate for the imbalanced representation of groups in both datasets. ROC of the classifier performance is displayed in Figure 22.

Accuracy (%)	65.53
Sensitivity (%)	75.00
Specificity (%)	56.06
AUC	0.75

Table 8: Performance of SVM classifier on the *beta weights* from ICA. The classifier was trained on the IKEM dataset and used to classify the *beta weights* of components from the NIHM dataset. The listed values were calculated with the consideration of weights.

4.4.2 Voxel-wise analysis

The classification based on the voxel-wise analysis required several steps to be performed on *beta weights* obtained from SPM on 158 subjects – 66 HC and 92 FES. First, the clustering of voxels to superpixels using SLIC learned on the training dataset is applied to the testing data. For each cluster, there is a mean of corresponding *beta weights* computed. Then, superpixel-means are transformed with the PLS transformation found on the training dataset.

The result of dimensionality reduction steps is then labeled by the classifier trained on the IKEM dataset. The classifier performance is listed in Table 9, and ROC is displayed in Figure 22.

f	**2**	**18**	**48**
Accuracy (%)	66.49	64.64	64.95
Sensitivity (%)	66.30	64.13	58.70
Specificity (%)	66.67	65.15	71.21
AUC	0.69	0.68	0.69

Table 9: Performance of SVM classifier with a different number of features (f).The classifier was trained on the IKEM dataset and used to classify the features obtained from the NIHM dataset. The performance measures were obtained from the results of leave-one-out cross-validation on the features from the voxel-wise analysis. The listed values were calculated with the consideration of weights.

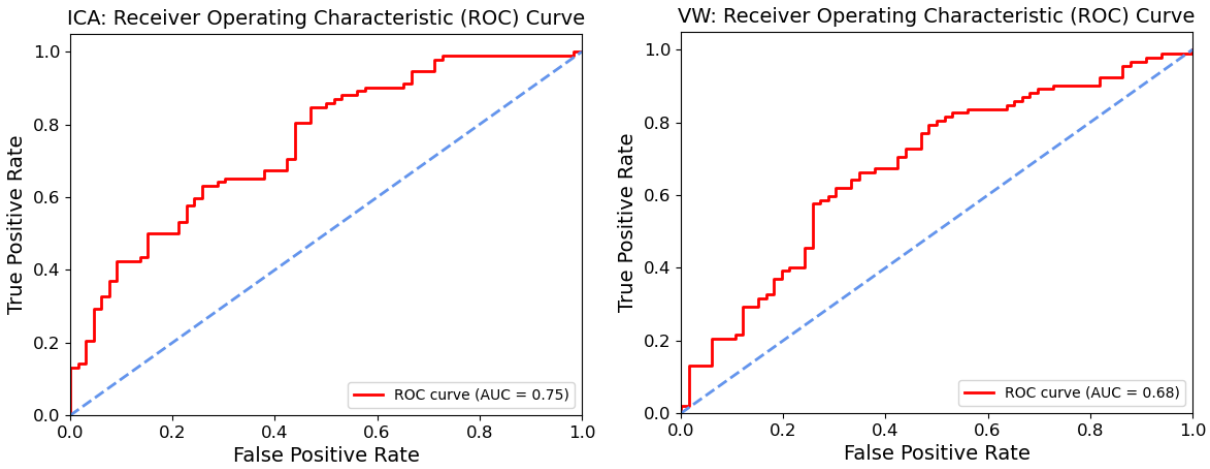

Figure 22: ROC curves obtained from the classification of the NIHM dataset when the classifier was trained on the IKEM dataset. On the left, the result of the classification of ICA *beta weights*. On the right, the result of the classification based on the *beta weights* from the voxel-wise analysis.

4.5 Regression

The regression task dealt with the explanation of the PANSS scale values with the *beta weights* obtained from the ICA or voxel-wise analysis. The prediction accuracy is measured with the coefficient of determination (R2), and root mean squared error (RMSE) calculated with the leave-one-out cross-validation results. The best performance was achieved with a polynomial kernel. Results of SVR with a polynomial kernel based on ICA *beta weights* are summarized in Table 10, and voxel-wise analysis-based results are listed in Table 11.

ICA			**Voxel-wise analysis**		
symptoms	**R2**	**RMSE**	**symptoms**	**R2**	**RMSE**
positive	0.04	3.82	positive	-3.95	8.34
negative	0.05	5.49	negative	-4.87	13.62
general	0.04	7.93	general	-3.08	16.17
total	0.08	14.03	total	-1.1	20.82

Table 10: Tables of regression results on ICA and voxel-wise analysis *beta weights* expressed as R2 and RMSE values for each symptom category.

The regression was approached with another method to check the previous results. In this case, the distance of each data point (*beta weight*) from the classification hyperplane was considered a feature. This procedure confirmed the previously obtained results, respectively it did not improve the prediction of PANSS values in any way.

symptoms	**R2**	**RMSE**
positive	-0.06	4.01
negative	-0.17	6.09
general	-0.06	8.32
total	-0.02	14.77

Table 11: Table of regression results on ICA *beta weights'* distances from the SVM classification hyperplane expressed as R2 and RMSE values for each symptom category.

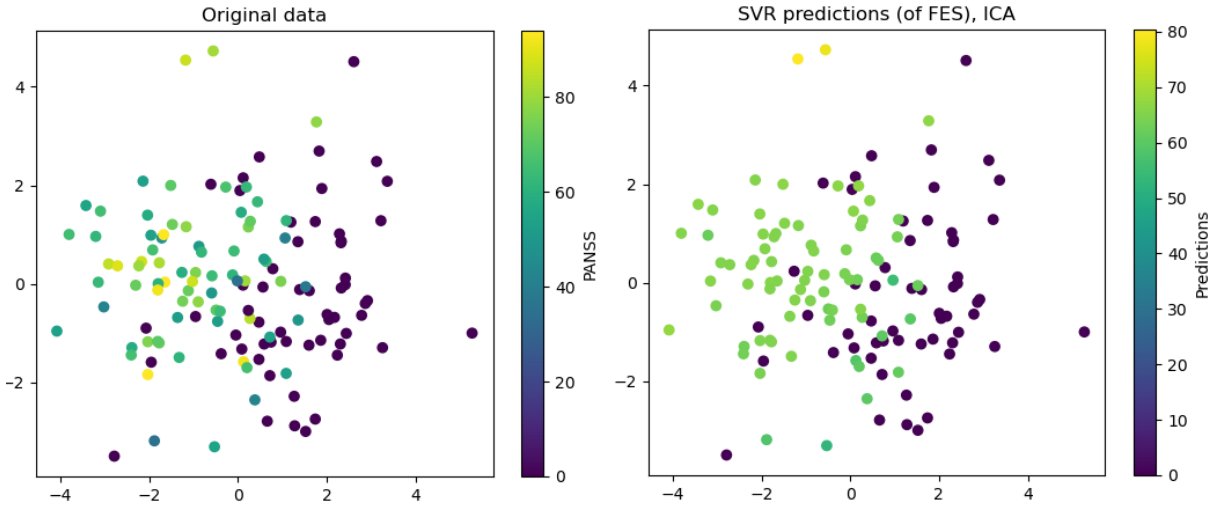

Figure 23: The result of the SVR with a polynomial kernel applied on the *beta weights* obtained from the ICA analysis to explain the PANSS scale. Left: PCA projection of the original data; the 0 values correspond to the HC group. Right: SVR predictions of the PANSS values (the HC group was not included in the regression process).

In addition, after taking the results into account, the hypothesis of the prediction of individual positive symptoms using *beta weights* was established and tested. The positive symptoms include delusions, conceptual disorganization, hallucinatory behavior, excitement, grandiosity, suspiciousness, and hostility. Neither this hypothesis was confirmed; the regression model behaved similarly as in the case of the sums of symptoms.

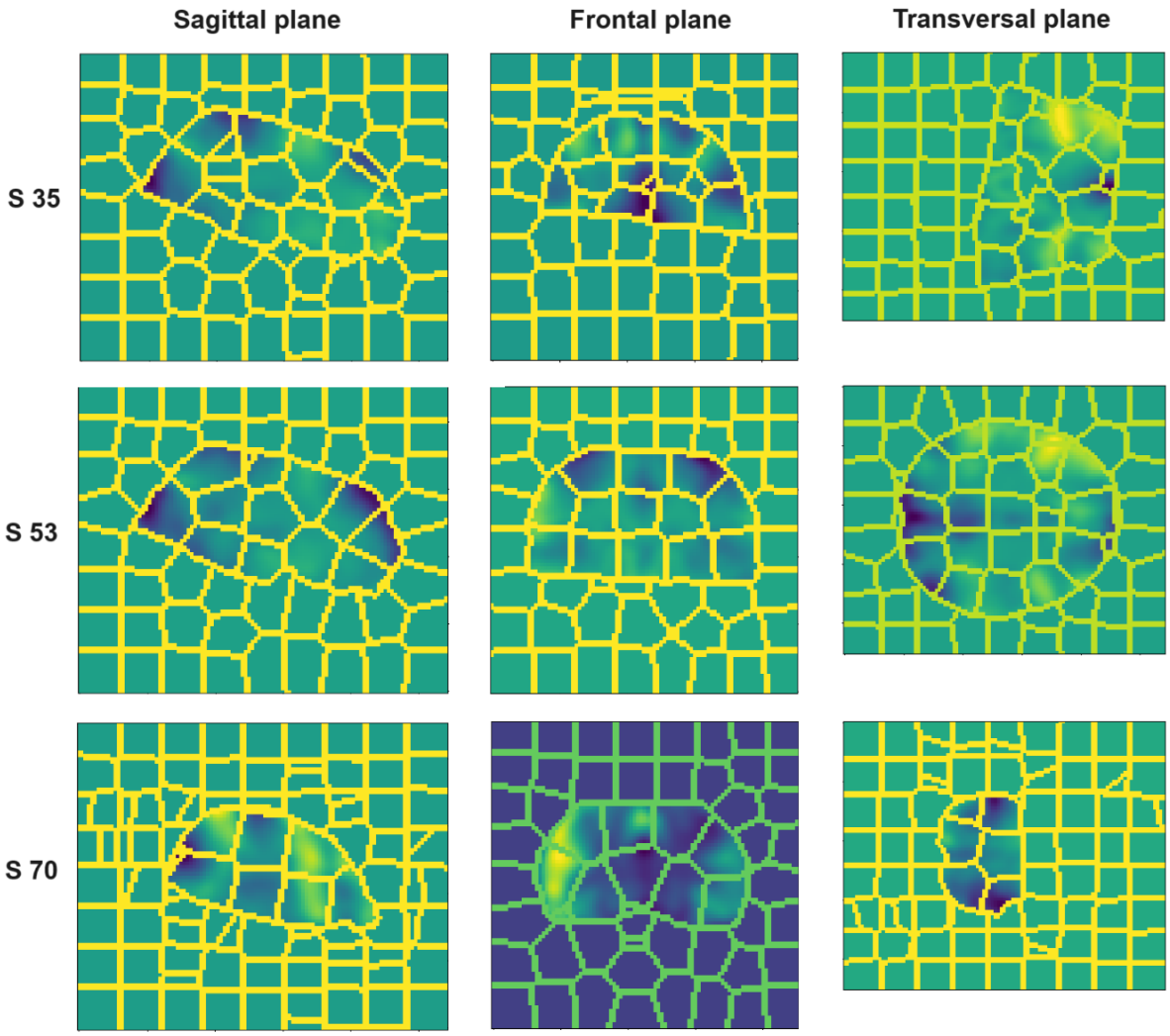

Figure 24: Demonstration of the clustering result using the SLIC superpixels. The result of the clustering of the two-channel image obtained as the mean of the *beta weights* across each group (FES, HC) separately is depicted as 3 slices (S) of the brain in the sagittal, frontal, and transversal plane. The yellow lines mark the borders of superpixels.

5 Discussion

5.1 Replication study

First, the replication study of [3] was conducted. Note that some of the replication methods were not exactly similar to the previous study due to their unnecessary complexity, as was mentioned in Section 3.

First, we shall discuss the results of the replication on the IKEM dataset. The independent component analysis (ICA) found a substantial correlation ($|r| > 0.5$) between the time course of the experiment and the mean (across subjects) activity of the component in 11 out of 35 estimated components. An additional two-sample t-test excluded another two components since there was no significant difference between the group of schizophrenia patients (FES) and healthy controls (HC). The components were subsequently identified, and the results were as follows: Positive correlation with the experiment was present for the visual cortex, middle frontal gyrus, inferior parietal lobule, and superior frontal gyrus. Besides the visual cortex, where the visual information is processed, the rest of the areas are responsible for cognitive control, motoric planning, and self-awareness. A negative correlation was found in the case of the medial prefrontal cortex, precuneal and cuneal cortex, anterior cingulate cortex (ACC), and parietal lobe. The precuneus, medial prefrontal cortex, and ACC are centers of self-awareness and self-reflection, and except for the auditory cortex, the components are parts of the default mode network (DMN).

In comparison to the study by Spaniel et al., there were estimated more significant independent components (3 in the case of the previous study, 9 in the replication with the IKEM dataset). The components that seemed to be very similar were:

- 2, marked as the anterior part of the DMN in the case of the study by Spaniel et al., and 7 – medial prefrontal cortex and ACC – also the anterior part of the DMN in the replication,

- 9, labeled as the posterior DMN in the previous study, and 15 in the replication study,

labeled as the precuneus, parietal lobe, and ACC are parts of the posterior and anterior DMN too,

- 23, identified as a part of the central executive network (CEN) in the case of the previous study, and 22, identified as the middle frontal gyrus (part of CEN) in the case of the replication.

The three components exhibited similar activations during the experiment. Both of the conclusions of the previous work were replicated on an enlarged dataset with a slightly different methodology. The conclusions stated that there was a significant difference between the FES and HC groups in the medial frontal gyrus and posterior cingulate gyrus; precisely, FES showed lower cortical activation in these areas. Another reported conclusion was that the self-other agency judgment is related to the dynamic switching of the DMN and CEN.

Nonetheless, there were differences in the results of [3] and the replication study. In the context of ICA, in the previous study, there were several significantly different components missing, e.g. the visual cortex. Besides the number of significant components from ICA, there were differences in the results of voxel-wise analyses. The previous study found significantly stronger activation only during the self-agency (SA) condition in the group of HC in comparison to FES. In the replication study, during the SA condition, HC exhibited stronger activation than FES in areas of posterior and anterior DMN in comparison to the OA condition. And during the OA condition, HC exhibited stronger activation than FES in the premotor cortex when compared to the SA condition.

After the evaluation of the IKEM dataset analysis, the same methods were applied to the NIHM dataset. The results of ICA were very different from the results obtained in the previous study and from the IKEM dataset. There were different brain areas positively correlated with the time course of the experiment estimated. In the case of negatively correlated components, there were a few components identified as similar brain areas as in the previous study.

As in the case of the IKEM dataset, the results of the voxel-wise analysis differ from the previous study. There was a stronger activation during the OA condition compared to the SA condition in the HC group than in the FES group. The difference between the IKEM

and NIHM datasets could be easily seen since, in the case of the NIHM dataset, there were very small significant clusters of voxels found, and in the case of the IKEM dataset, the clusters aligned with a sufficient part of the premotor cortex. During the SA condition, when compared to the OA condition, HC exhibited stronger activation than FES in the anterior and posterior DMN on smaller areas than in the IKEM dataset.

5.2 Classification of the IKEM dataset

The two performed analyses (ICA and the voxel-wise analysis), the *beta weights* obtained from them, respectively, were further used for the classification between the FES and HC groups. The *beta weights* from ICA were used directly – they were fed to the classifier within the leave-one-out cross-validation. The accuracy of the model was 78.16%, sensitivity 76.32%, and specificity 80.00%. The area under the receiver operating curve AUC was 0.85. The performance was subsequently compared to the performance on the *beta weights* obtained from the voxel-wise analysis.

Before the second classification took place, there had to be several dimensionality-reduction steps performed on the *beta weights*. First, clustering with the SLIC superpixels was carried out. The superpixels' means were then transformed with the partial least squares transformation. The optimal number of features was searched, and the classification was performed for several values of this hyperparameter (2, 18, 48) for two reasons: first, the dependence of the model accuracy on the number of features was a noisy function with several local optima; secondly, the fact that the search is performed on the whole dataset that is further used for the classification task implies a form of overfitting of the model. Nonetheless, there was no dataset part set aside for this purpose because of the insufficient size of the IKEM dataset.

The features obtained from *beta weights* were fed to the classifier. The results of leave-one-out cross-validation were reported for the number of features $f = 2, 18, 48$. The model achieved a relatively high performance that was very similar for 18 and 48 features; the accuracy, sensitivity, and specificity were about $80 - 83\%$ in both cases. The performance for only 2 features was surprisingly not much worse, all three measures about 75%.

5.3 Classification of the NIHM dataset

The classification task was evaluated on the NIHM dataset such that the trained classifier (trained on the IKEM dataset) was used to classify the NIHM data. The performance of both models, whether it was the ICA classification model or the voxel-wise analysis classification model, was worse than in the case of the leave-one-out cross-validation on the IKEM dataset.

The ICA *beta weights* were obtained on the merged IKEM and NIHM datasets for this particular task in order to have the same independent components fed to the classifier from both datasets. Another option would be to use the ICA transformation matrix found on the IKEM dataset and apply it to the NIHM data. This would provide a simple way to classify 'new' subjects and also provide further insight into how transferable the results of the analysis based on this experiment are between subjects. The question remains whether this transformation would need to be obtained on a larger dataset than the IKEM dataset in this study. This method is certainly worth further investigation. In the case of ICA *beta weights*, the accuracy of the model was 65.53%, sensitivity 75.00%, specificity 56.06%, and AUC 0.75.

Before the classification based on the voxel-wise analysis, the *beta weights* had to be transformed to lower-dimensional space. In this case, SLIC superpixels clustering trained on the IKEM dataset was applied to the NIHM data. Then, the means of superpixels were calculated and transformed with the partial least squares transformation matrix learned on the IKEM dataset. Obtained features were fed to the classifier trained on the IKEM dataset for classification.

In the case of the voxel-wise analysis, the performance measures ranged in similar values as for the ICA classification. For all tested numbers of features, the accuracy was about 65%. Sensitivity and specificity were balanced for 2 and 18 features; for 48 features, the specificity outweighed the sensitivity of the model.

The fact that the classifiers perform worse in the case of the NIHM dataset is apparent from the results of the analyses themselves. It is evident that the estimated components differ when comparing the IKEM and NIHM analyses results. This can be caused by a different MRI machine, their different age range and sex representation, or other general factors that

accompany the fact that the measurements took place in different centers, even though all of the formal criteria of the experiment stayed the same.

5.4 Regression

Support vector regression was used to predict the values of the PANSS scale. The prediction was performed based on the *beta values* obtained either from the ICA or the voxel-wise analysis within the leave-one-out cross-validation. Although the prediction was tried with different approaches, none of them led to a successful result.

The inability to predict the PANSS values using the described methods may arise from the fact that simple models, such as support vector regression, are not sufficient to explain the PANSS scale. On the other hand, it is also possible that even more complex methods would not achieve the results either because the PANSS scale may not be explainable with fMRI data.

6 Conclusion

The replication study of [3] in which the group of first-episode schizophrenia patients (FES) and healthy controls (HC) were compared using the Self-agency experiment was conducted. The study was carried out on an enlarged sample and on another fully independent sample that was, in addition, obtained from a different MRI center. The comparison was based on the results of the independent component analysis and the voxel-wise (SPM) analysis. The results of the replication were in some respects consistent with the previous study but differed in other aspects. It managed to confirm that there exists a significant difference between the FES and HC groups; FES patients exhibited lower cortical activation in the areas of the default mode network (DMN). The explored self-agency judgment was found to be related to the dynamic switching of the DMN and the central executive network. Nonetheless, in this study, there were other significantly different areas of the brain identified; the most prominent were areas of the cuneal and visual cortex.

The results of both analyses (ICA and voxel-wise) were subsequently used for classification. When using only one (IKEM) dataset, the performance of models, once using the ICA results and once using the voxel-wise analysis results, were approximately similar; the voxel-wise based learning was slightly more sufficient. A solid accuracy of approximately 80% was achieved. When the model trained on the IKEM dataset was used to classify the data from the other (NIHM) dataset, the performance of the model was less sufficient. The reason may be the different MRI machines used for the measurement or different groups' distributions in the two datasets.

Additionally, the results of the mentioned analyses were used to explain the PANSS scale [5]. The used methods failed to explain the PANSS values. It is worth further exploration to figure out whether there are methods that would help to solve this problem or whether the PANSS scale is not explainable with fMRI data obtained from this experiment.

References

[1] Krishna R. Patel, Cherian Jessica, Kunj Gohil, and Dylan Atkinson. Schizophrenia: Overview and treatment options, 2014.

[2] Christopher A. Ross, Russell L. Margolis, Sarah A.J. Reading, Mikhail Pletnikov, and Joseph T. Coyle. Neurobiology of schizophrenia, 2006.

[3] Filip Spaniel, Jaroslav Tintera, Jan Rydlo, Ibrahim Ibrahim, Tomas Kasparek, Jiri Horacek, Yuliya Zaytseva, Martin Matejka, Marketa Fialova, Andrea Slovakova, Pavol Mikolas, Tomas Melicher, Natalie Görnerova, Cyril Höschl, and Tomas Hajek. Altered neural correlate of the self-agency experience in first-episode schizophrenia-spectrum patients: An fmri study. *Schizophrenia Bulletin*, 42:916–925, 7 2016.

[4] Michael J. Owen, Akira Sawa, and Preben B. Mortensen. *Schizophrenia*, volume 388. Lancet Publishing Group, 2016.

[5] Chantelle J. Giesbrecht, Norm O'Rourke, Olga Leonova, Verena Strehlau, Karine Paquet, Fidel Vila-Rodriguez, William J. Panenka, G. William MacEwan, Geoffrey N. Smith, Allen E. Thornton, and William G. Honer. The positive and negative syndrome scale (panss): A three-factor model of psychopathology in marginally housed persons with substance dependence and psychiatric illness. *PLoS ONE*, 11, 2016.

[6] Chris D Frith, Sarah-Jayne Blakemore, and Daniel M Wolpert. Interactive report explaining the symptoms of schizophrenia: Abnormalities in the awareness of action 1, 2000.

[7] Daniel R. Weinberger and Paul J. Harrison. *Schizophrenia*. Wiley, 2010.

[8] R. S. Kahn and I. E. Sommer. The neurobiology and treatment of first-episode schizophrenia, 2015.

[9] Peter J Weiden, Peter F Buckley, and Michael Grody. Understanding and treating "first-episode" schizophrenia. *Psychiatric Clinics of North America*, 30:481–510, 2007.

[10] Georg Northoff and Felix Bermpohl. Cortical midline structures and the self. *Trends in Cognitive Sciences*, 8:102–107, 2004.

[11] Vesa Kiviniemi, Tuomo Starck, Jukka Remes, Xiangyu Long, Juha Nikkinen, Marianne Haapea, Juha Veijola, Irma Moilanen, Matti Isohanni, Yu Feng Zang, and Osmo Tervonen. Functional segmentation of the brain cortex using high model order group pica. *Human Brain Mapping*, 30:3865–3886, 2009.

[12] Randy L. Buckner, Jessica R. Andrews-Hanna, and Daniel L. Schacter. The brain's default network: Anatomy, function, and relevance to disease, 2008.

[13] Pierre Comon. Signal processing independent component analysis, a new concept?*, 1994.

[14] A Hyvärinen and E Oja. Independent component analysis: algorithms and applications, 2000.

[15] Thomas M. Cover and Joy A. Thomas. *Elements of Information Theory*. Wiley, 2005.

[16] Zhenyi An. Different estimation methods for the basic independent different estimation methods for the basic independent component analysis model component analysis model, 2018.

[17] Johan Himberg, Aapo Hyvärinen, and Fabrizio Esposito. Validating the independent components of neuroimaging time series via clustering and visualization. *NeuroImage*, 22:1214–1222, 2004.

[18] Karl J. Friston, John T. Ashburner, Stefan J. Kiebel, Thomas E. Nichols, and William D. Penny. *Statistical Parametric Mapping*. Elsevier, 2007.

[19] Radhakrishna Achanta, Appu Shaji, Kevin Smith, Aurelien Lucchi, Pascal Fua, and Sabine Süsstrunk. Slic superpixels, 2010.

[20] Paul Geladi and Bruce R Kowalski. Partial least-squares regression: A tutorial, 1986.

[21] Dante M Pirouz and Doctoral Student. An overview of partial least squares, 2006.

[22] Matthew Barker and William Rayens. Partial least squares for discrimination. *Journal of Chemometrics*, 17:166–173, 2003.

[23] Corinna Cortes, Vladimir Vapnik, and Lorenza Saitta. Support-vector networks editor, 1995.

[24] Olivier Chapelle, Patrick Haffner, and Vladimir N Vapnik. Support vector machines for histogram-based image classification, 1999.

[25] Christopher J C Burges. A tutorial on support vector machines for pattern recognition, 1998.

[26] Alex J Smola, Bernhard Sch¨olkopf, and Sch¨ Sch¨olkopf. A tutorial on support vector regression *, 2004.

[27] Lars Rosenbaum, Alexander Dörr, Matthias R. Bauer, Frankmboeckler, and Andreas Zell. Inferring multi-target qsar models with taxonomy-based multi-task learning. *Journal of Cheminformatics*, 5, 2013.

[28] D V Sheehan, Y Lecrubier, K H Sheehan, P Amorim, J Janavs, E Weiller, T Hergueta, R Baker, and G C Dunbar. The mini-international neuropsychiatric interview (m.i.n.i.): the development and validation of a structured diagnostic psychiatric interview for dsm-iv and icd-10. *The Journal of clinical psychiatry*, 59 Suppl 20:22–33;quiz 34–57, 1998.

[29] Wellcome Trust Centre for Neuroimaging. Spm12 (statistical parametric mapping): The analysis of functional brain images), 2014.

[30] Xiangrui Li, Paul S Morgan, John Ashburner, Jolinda Smith, and Christopher Rorden. The first step for neuroimaging data analysis: Dicom to nifti conversion. *Journal of neuroscience methods*, 264:47–56, 2016.

[31] A. Nieto-Castanon. Handbook of functional connectivity magnetic resonance imaging methods in conn. *Boston, MA: Hilbert Press*, 2020.

[32] N. Tzourio-Mazoyer, B. Landeau, D. Papathanassiou, F. Crivello, O. Etard, N. Delcroix, B. Mazoyer, and M. Joliot. Automated anatomical labeling of activations in spm using a macroscopic anatomical parcellation of the mni mri single-subject brain. *NeuroImage*, 15:273–289, 2002.

[33] V. D. Calhoun. A method for making group inferences using independent component analysis of functional mri data: Exploring the visual system. *NeuroImage*, S88, 2001.

[34] Yuhui Du. Neuromark: An automated and adaptive ica based pipeline to identify reproducible fmri markers of brain disorders. *NeuroImage: Clinical*, 28, 2020.

Appendix

C no.	SI	r	t
1	0.97	-0.49	-4.83
2	0.97	0.22	0.65
3	0.98	-0.31	0.48
4	0.97	-0.14	1.49
5	0.97	0.70	0.85
6	0.98	-0.17	-0.72
7	0.97	-0.65	-6.23
8	0.98	0.15	0.86
9	0.97	-0.23	-6.23
10	0.97	0.53	3.91
11	0.97	0.20	6.99
12	0.97	-0.16	2.28
13	0.97	0.00	0.72
14	0.97	0.15	-2.10
15	0.97	-0.80	-7.42
16	0.97	-0.61	-0.46
17	0.98	0.39	1.89
18	0.97	0.34	0.33
19	0.96	-0.72	-5.48
20	0.97	0.66	2.40
21	0.97	-0.25	3.56
22	0.97	0.75	7.13
23	0.95	-0.17	1.29
24	0.97	0.78	3.32
25	0.96	0.25	3.80
26	0.97	0.43	-1.65
27	0.96	-0.48	-6.85
28	0.94	-0.17	1.42
29	0.95	0.43	1.67
30	0.95	-0.72	-2.60
31	0.93	0.64	3.43
32	0.94	0.37	2.97
33	0.92	0.10	5.16
34	0.93	-0.32	2.96
35	0.83	-0.10	-3.17

C no.	SI	r	t
1	0.98	0.21	-1.37
2	0.97	-0.50	-0.86
3	0.97	-0.64	-0.05
4	0.97	0.01	-0.98
5	0.97	-0.58	-4.87
6	0.96	-0.14	0.19
7	0.97	-0.26	-0.38
8	0.97	0.10	-0.12
9	0.96	0.13	2.30
10	0.98	0.21	2.38
11	0.97	-0.23	-1.11
12	0.97	-0.73	-4.11
13	0.96	-0.11	-2.26
14	0.97	0.39	3.91
15	0.96	-0.13	1.53
16	0.96	0.17	1.14
17	0.97	-0.20	0.36
18	0.96	-0.64	-3.53
19	0.96	-0.47	-2.02
20	0.93	0.80	5.76
21	0.92	-0.29	-2.64
22	0.94	0.55	2.95
23	0.93	0.58	3.53
24	0.89	0.33	1.12
25	0.85	-0.57	-3.74
26	0.83	0.75	4.34
27	0.81	0.60	1.35
28	0.81	-0.78	-3.41
29	0.87	0.43	1.30
30	0.91	0.51	3.08
31	0.78	0.73	5.51
32	0.88	-0.08	-1.09
33	0.80	0.69	4.01
34	0.76	0.42	2.22
35	0.58	-0.32	-0.28

C no.	SI	r	t
1	0.96	0.50	7.12
2	0.97	-0.40	-5.20
3	0.98	-0.08	3.36
4	0.97	-0.33	-0.45
5	0.97	-0.54	-6.27
6	0.97	-0.53	-2.25
7	0.97	-0.07	-2.27
8	0.97	0.53	2.64
9	0.97	-0.22	-2.25
10	0.95	-0.33	0.16
11	0.97	0.09	2.31
12	0.97	0.04	-3.83
13	0.97	0.41	2.12
14	0.96	0.25	4.21
15	0.96	-0.02	2.45
16	0.95	0.59	3.19
17	0.97	-0.62	-7.23
18	0.94	0.79	6.03
19	0.97	-0.41	-3.46
20	0.97	0.60	5.30
21	0.97	-0.72	-4.93
22	0.96	0.77	8.99
23	0.96	0.17	-0.72
24	0.97	0.36	3.17
25	0.95	0.50	4.76
26	0.96	-0.84	-7.07
27	0.96	0.02	2.78
28	0.95	0.22	4.23
29	0.96	-0.40	2.34
30	0.93	-0.51	-0.83
31	0.92	-0.68	-1.33
32	0.95	-0.40	-3.92
33	0.80	-0.60	-3.75
34	0.92	0.81	4.73
35	0.64	-0.76	-5.74

Figure 25: Tables of results of the significant components selection performed on – from left – IKEM, NIHM, and merged datasets. The criteria were stability index (SI), correlation value (r), and t value obtained from a two-sample t-test (t). Components in blue passed all tests as significant; components in orange did not pass the two-sample t-test but are included as features in the classification task.